A Thesis

entitled

Structural Analyses of Lipid A from *Burkholderia pseudomallei* and *Burkholderia thailandensis* by Mass Spectrometry

by

Ravi Chandran Reddy Alla

Submitted to the Graduate Faculty as partial fulfillment of the requirements for the

Master of Science Degree in Chemistry

_____
Dr. Dragan Isailovic, Committee Chair

_____
Dr. Jon Kirchhoff, Committee Member

_____
Dr. Donald Ronning, Committee Member

_____
Dr. Patricia Komuniecki, Dean
College of Graduate Studies

The University of Toledo

December 2015

An Abstract of

Structural Analyses of Lipid A from *Burkholderia pseudomallei* and

Burkholderia thailandensis by Mass Spectrometry

by

Ravi Chandran Reddy Alla

Submitted to the Graduate Faculty as partial fulfillment of the requirements for the Master of Science Degree in Chemistry

The University of Toledo

December 2015

Burkholderia pseudomallei is an infectious bacterium, which causes a lethal disease, melioidosis, and has potential for misuse as a bioweapon. The cell wall of this bacterium contains lipopolysaccharides (LPSs). A component of LPS is a phosphorylated glycolipid known as lipid A, which may be responsible for pathogenic properties of *B. pseudomallei*. Therefore, the studies about the structure of lipid A and the influence of lipid A on the virality of *B. pseudomallei* are important.

Here, lipid A species originating from *B. pseudomallei* strain 1026b and avirulent *B. thailandensis* strain E264 were structurally characterized by mass spectrometry (MS) and their lipid A profiles were compared as well. An earlier study by Novem et al. on lipid A from *B. pseudomallei* strain KHW and *B. thailandensis* strain ATCC 700388 revealed that a lipid A species with a mass-to-charge ratio (*m/*z) of 973.59 (z=-2) was different between the two bacteria, and a hypothetical structure of this *B. pseudomallei*-specific ion was proposed. In order to further investigate the structural differences of lipid

A between *B. pseudomallei* and *B. thailandensis*, MALDI-MS and ESI-MS were used in this study.

The lipid A samples were isolated from *B. pseudomallei* 1026b and *B. thailandensis* E264 using a hot phenol-water extraction protocol. After liquid-liquid extraction into a chloroform/methanol phase, lipid A species were analyzed by MALDI-MS (using mostly 6-aza-2-thiothymine (ATT) as the matrix) and ESI-MS in negative ion mode, while tandem mass spectrometry (MS/MS) was used for structural investigation of lipid A ions. Additionally, partial and complete O-deacylation of lipid A samples were achieved using ammonium hydroxide and methylamine solutions, respectively, in order to study structures of lipid A acyl chains.

MALDI-MS of lipid A from *B. pseudomallei* 1026b and *B. thailandensis* E264 confirmed that an ion with an *m/z* value of 1580.040 (z=-1) was detected only in *B. pseudomallei* 1026b. Since deprotonated lipid A corresponding to this *m/z* was not found in the literature and available lipid structure databases, the structure of this and other deprotonated lipid A species were studied further using MALDI and ESI-MS/MS.

In the MALDI-MS/MS data of the lipid A ion with an *m/z* value of 1580.040, a peak at *m/z* value of 1444.023 was detected that was also seen in a MALDI-MS spectrum of a lipid A sample from *B. pseudomallei* 1026b. Based on this, it was hypothesized that the lipid A ion with an *m/z* of 1580.040 could be a structural modification of 136 mass units on the lipid A structure of the ion with an *m/z* of 1444.023. Two parent structures were proposed for the lipid A ion with an *m/z* value of 1580.040. However, the possibility of having different structural isomers makes it difficult to propose, or to confirm, an exact

parent structure of the lipid A ion with an *m/z* of 1580.040. Additionally, the presence of phosphorylated species with *m/z* values of ~79 (PO_3^-) and 97 ($H_2PO_4^-$) and pyrophosphorylated species with *m/z* values of ~ 159 ($HP_2O_6^-$) and 176 ($H_3P_2O_7^-$) indicated that this lipid A structure likely contains two phosphoryl residues.

To further study the structures of lipid A species from *B. pseudomallei* 1026b, partial and complete O-deacylation of lipid A samples were performed. MALDI-MS spectra obtained after partial O-deacylation of lipid A samples showed intense ions with *m/z* values of 1137.712 and 1217.639, while peaks at 927.591 and 1007.548 were detected after complete O-deacylation. MALDI-MS/MS studies of O-deacylated lipid A revealed the identity of the O-acyl chains in *B. pseudomallei* lipid A that were proposed previously by Novem et al. The structures of these species also show the presence of $C_{16:0}$ acyl chains attached to the sugar moieties by an amide linkage at positions 2 and 2′ of the two glucosamines.

In summary, a lipid A ion with an *m/z* of 1580.040, which is unique to *B. pseudomallei* 1026b, was detected and structurally characterized by MALDI and ESI-MS analysis in this study. This lipid A is likely a biphosphorylated glycolipid containing five acyl chains attached to two glucosamines. However, an exact structure of this glycolipid and its potential influence on the virulence of *B. pseudomallei* 1026b remains to be determined in future studies.

I would like to dedicate this thesis to my beloved mom and dad for bearing with me all these years and supporting me in every possible way.

Acknowledgements

I have to be thankful to a lot of people. I would first like to thank my advisor, mentor and father figure, Dr. Dragan Isailovic for his help over two and a half years. Dr. Dragan taught me about mass spectrometry from the beginning and he did that very patiently. I will be forever indebted to him.

I thank Dr. Jon Kirchhoff and Dr. Donald Ronning for being part of my research committee and for their useful advices regarding the content of this thesis.

I would like to thank Dr. Mark Wooten and Dr. Michael Bechill for their ideas and help with this project. I would also like to thank Austen Mance, Susan Salari and Kevin Samson for their help with the analysis of lipid A.

I would like to thank Dr. Leif Hansen and Dr. Yong Wah Kim for training me on MS instruments. I would also like to thank Youming Cao and Thomas Kina for fixing our Q-TOF mass spectrometer, whenever we had a problem. I would like to convey my special thanks to Dr. Edith Kippenhan. She taught me so many new things about teaching and life. I would like to thank all my lab mates, past and current: Raymond, Rachel, Siddhita, Sanjeevani, Krishani, Steven and Justin.

Last but not the least, my family; Mom and Dad, I am so grateful to you for your support. I would also like to take this as an opportunity to thank all my friends.

Table of Contents

Abstract iii

Acknowledgements vii

Table of Contents viii

List of Tables x

List of Figures xi

List of Abbreviations xiv

List of Symbols xvii

1 Introduction 1

1.1 *Burkholderia pseudomallei* and *Burkholderia thailandesis*, Gram-negative Bacteria 1

1.2 Mass Spectrometry 3

1.2.1 MALDI Mass Spectrometry 5

1.2.2 ESI Mass Spectrometry 9

1.2.2.1 Mechanisms of Ion Formation in ESI 12

1.3 Lipopolysaccharides 13

1.4 MALDI-MS Analysis of Lipid A 17

1.5 ESI-MS Analysis of Lipid A 18

2 Materials and Methods....21
2.1 Isolation of Lipid A....21
2.1.1 Materials for Lipid A Isolation....21
2.1.2 Lipopolysaccharide and Lipid A Isolation Protocol....21
2.2 *O*-deacylation of Lipid A (Partial and Complete *O*-deacylation)....23
2.3 Mass Spectrometry of Lipid A....24
2.3.1 Materials....24
2.3.2 MS Experiments....24
3 Results....26
3.1 MALDI-MS and MALDI-MS/MS Analysis of Lipid A from *B. pseudomallei* Strain 1026b and *B. thailandensis* Strain E264....26
3.2 MALDI-MS and MALDI MS/MS Analysis of O-deacylated Lipid A....42
3.3 ESI-MS, ESI-MS/MS, and ESI MS/MS/MS Analysis of Lipid A....49
4 Conclusions and Future Work....54
4.1 Conclusions....54
4.2 Future Work....56
References....58
A LC-MS Study of Lipid A from *B. pseudomallei*....66
References....74

List of Tables

1.1 Different Types of Lasers Used in MALDI-MS and Their Wavelengths 6

1.2 Type of Matrices Used for Different Types of Biomolecules in MALDI-MS 9

3.1 Experimental and Theoretical Masses of Each Lipid A Ion from *B. thailandensis* E264 and *B. pseudomallei* 1026b Along with Their Composition 32

List of Figures

1-1 Schematic of a mass spectrometer 4

1-2 Principle of MALDI-TOF MS 7

1-3 Schematic of MALDI-MS 8

1-4 Principle of ESI-MS....10

1-5 General structure of a lipopolysaccharide....14

1-6 General structure of lipid A 16

1-7 Hypothetical structure proposed by Novem et al.....19

3-1 MALDI-MS spectrum of lipid A from *B. pseudomallei* 1026b....28

3-2 MALDI-MS spectrum of lipid A from *B. thailandensis* E264 30

3-3 MALDI-MS/MS spectrum of ion with an *m/z* of 1801.231 of lipid A from *B. pseudomallei* 1026b 33

3-4 MALDI-MS/MS spectrum of ion with an *m/z* of 1670.135 of lipid A from *B. pseudomallei* 1026b 34

3-5 Fragmentation mechanisms: (A) Charge-driven fragmentation (B) Charge-remote fragmentation 36

3-6 MALDI-MS/MS spectrum of ion with an *m/z* of 1363.993 of lipid A from *B. pseudomallei* 1026b 37

3-7 MALDI-MS/MS spectrum of ion with an *m/z* of 1580.040 of lipid A from *B. pseudomallei* 1026b 38

3-8 MALDI-MS/MS spectrum of ion with an *m/z* of 1443.968 of lipid A from *B. pseudomallei* 1026b 39

3-9 Hypothetical structure of parent molecule of lipid A ion an with of *m/z* value of 1580.040 from *B. pseudomallei* 1026b 41

3-10 MALDI-MS spectrum of lipid A from *B. pseudomallei* 1026b after complete *O*-deacylation 43

3-11 MALDI-MS/MS spectrum of ion with an *m/z* of 927.591 of lipid A from *B. pseudomallei* 1026b after complete *O*-deacylation 44

3-12 MALDI-MS/MS spectrum of ion with an *m/z* of 1007.548 of lipid A from *B. pseudomallei* 1026b after complete *O*-deacylation 45

3-13 MALDI-MS spectrum of lipid A from *B. pseudomallei* 1026b after partial *O*-deacylation 46

3-14 MALDI-MS/MS spectrum of ion with an *m/z* of 1137.712 of lipid A from *B. pseudomallei* 1026b after partial *O*-deacylation 47

3-15 MALDI-MS/MS spectrum of ion with an *m/z* of 1217.639 of lipid A from *B. pseudomallei* 1026b after partial *O*-deacylation 48

3-16 High resolution ESI-MS spectrum of lipid A from *B. pseudomallei* 1026b 49

3-17 High resolution ESI-MS/MS spectrum of ion with an *m/z* of 1580.022 of lipid A from *B. pseudomallei* 1026b 51

3-18 Q-TOF-ESI-MS/MS spectrum of ion with an *m/z* of 789.5062 of lipid A from *B. pseudomallei* 1026b 52

A-1 LC-MS chromatogram of lipid A from *B. pseudomallei* 1026b 67

A-2 Extracted ion chromatogram of lipid A ion with an *m/z* of ~1364 from *B. pseudomallei* 1026b 68

A-3 LC-MS spectrum of lipid A ion with an *m/z* of ~1364 from *B. pseudomallei* 1026b 69

A-4 Extracted ion chromatogram of lipid A ion with an *m/z* of ~1580 from *B. pseudomallei* 1026b 70

A-5 LC-MS spectrum of lipid A ion with an *m/z* of ~1580 from *B. pseudomallei* 1026b 71

A-6 Extracted ion chromatogram of lipid A ion with an *m/z* of ~1801from *B. pseudomallei* 1026b 72

A-7 LC-MS spectrum of lipid A ion with an *m/z* of ~1801 from *B. pseudomallei* 1026b 73

List of Abbreviations

ATT.....6-aza-2-thiothymine

B.....Magnetic sector

CI.....Chemical ionization
CID.....Collision induced dissociation
CEM.....Channel electron multiplier
CHCA .....Alpha cyano-4-hydroxycinnamic acid
CH_3NH_2 .....Methylamine
CRM.....Charge residue model

DHB .....Dihydroxy benzoic acid
DI H_2O .....Deionized water
DIT.....Dithranol
DNase.....Deoxyribonuclease

E .....Electric sector
EI.....Electron ionization
Er:YAG .....Erbium-doped yttrium aluminum garnet
ESI-MS .....Electrospray ionization mass spectrometry
EtOH .....Ethyl alcohol

FAB.....Fast atom bombardment
FT-ICR.....Fourier transform ion cyclotron resonance

GlcN I.....Glucosaminyl residue
GlcN II .....Glucosamine group
Glc*p*N.....2-amino-2-deoxy-glucopyranose
Glc*p*N3N 2, 3-diamino-2, 3-deoxy-glucopyranose

HPA .....3-Hydroxypicolinic acid
HPLC .....High performance liquid chromatography
HPO_3 and H_3PO_4.....Phosphoryl residues

ICP .....Inductively coupled plasma

ICR.....Ion cyclotron resonance
IEM .....Ion evaporation model
IR.....Infrared

Kdo.....3-deoxy-D-manno-oct-2-ulosonic acid

LAL.....Limulus amebocyte lysate
LB .....Luria Bertani Broth
LC-MS .....Liquid chromatography-mass spectrometry
LD .....Laser desorption
LDMS .....Laser desorption mass spectrometry
LID.....Laser induced dissociation
LIT .....Linear ion trap
LPS.....Lipopolysaccharide

MALDI-MS .....Matrix assisted laser desorption/ionization mass spectrometry
MALDI-TOF MS.....Matrix-assisted laser desorption/ionization time-of-flight mass spectrometry
MCP .....Microchannel plate
MS .....Mass spectrometry
MS/MS .....Tandem mass spectrometry

NH_4OH.....Ammonium hydroxide
Nd:YAG.....Neodymium-doped yttrium aluminum garnet
NMR .....Nuclear magnetic resonance

OPS .....O-specific polysaccharide
OS .....Oligosaccharide

PBS .....Phosphate buffered saline

QIT.....Quadrupole ion trap

RNase.....Ribonuclease
R-type LPS.....Rough lipopolysaccharide

SA .....Sinapic acid
SIMS .....Secondary ion mass spectrometry
S-type LPS .....Smooth lipopolysaccharide
SR-type LPS .....Semi-rough lipopolysaccharide

TEA.....Triethanolamine
THAP .....Trihydroxyacetophenone
TOF .....Time-of-flight

Tris-HCl.....Tris hydrochloride

UV.....Ultraviolet
UVPD.....Ultraviolet photon dissociation

List of Symbols

m/z	Mass-to-charge ratio
m	Mass
z	Charge state
e	Elementary charge
U	Potential difference
t	Time-of-flight to the detector
L	Length of drift tube
q	Charge
ε	Electrical permittivity of the surrounding medium
γ	Surface tension of the solvent
R	Radius of the droplet
M	Molar mass

Chapter 1

Introduction

1.1 *Burkholderia pseudomallei* and *Burkholderia thailandensis*, Gram-negative Bacteria

Burkholderia pseudomallei is an infectious Gram-negative bacterium, which causes the lethal disease melioidosis, and has potential for misuse as a bioweapon.[1] *B. pseudomallei* is commonly found in the soil and water across Southeast Asia and Northern Australia. Symptoms of melioidosis include chronic abscesses and acute septicemia.[2] Several studies have been performed on melioidosis patients to prove that this disease is non-contagious. It is only spread by inhalation and ingestion of bacterium or by skin inoculation.[3] Additional research has been devoted to the analysis of structural and functional relationships between *B. pseudomallei* and genetically similar, but aviral species such as *Burkholderia thailandensis*.[1, 4]

Due to the ability of bacterial lipopolysaccharides (LPSs) to induce an immune response in a host organism, the structural analysis of LPSs found in the *B. pseudomallei* cell wall is important.[5] Typically, an LPS has three domains: a hydrophilic polysaccharide chain (O-antigen), the intermediate core oligosaccharide, and a

hydrophobic lipid A moiety.[6] Lipid A contains a disaccharide backbone consisting of glucosamines with phosphoryl residues (PO_3^-, $H_2PO_3^-$), arabinoses (Ara4N), and acyl chains attached. Due to the amphiphilic nature of lipid A, separation and analytical characterization (e.g., desolvation and ionization) of lipid A are challenging processes.[7-10]

It was proposed that *B. pseudomallei* may dysregulate the host immune response via properties inherent to the lipid A produced by this bacterium.[1] Additionally, endotoxin activity of LPS can be modified by acylation, phosphorylation and glycosylation of lipid A.[6] Structural determination of lipid A can help in understanding the effects of *B. pseudomallei* LPS on inflammatory activities on a molecular level.[1] While other techniques such as NMR have been attempted for the structural characterization of lipid A,[11] mass spectrometry (MS) is a more sensitive technique, which is suitable for structural characterization of heterogeneous and complex lipid A samples.

Early MS studies on lipid A were mostly performed using laser desorption mass spectrometry (LDMS).[8, 11] Other techniques such as fast atom bombardment mass spectrometry (FAB)[12], and liquid secondary ion mass spectrometry (SIMS)[13], were also applied for analysis of lipid A. Later on, ESI-MS and MALDI-MS became efficient tools in determining the structures of lipid A from different strains of Gram-negative bacteria.[10, 14-20] More recently, ultraviolet photon dissociation (UVPD) mass spectrometry has been used to obtain information about the fragments of lipid A, and thus made the structural analysis simpler.[7, 21]

A recent study examined the structures of lipid A from *B. pseudomallei* and *B. thailandensis* using ESI-MS.[1] This study revealed the heterogeneous nature of lipid A and proposed a hypothetical structure of lipid A that can be used to assign lipid A ions found in these species. While most ions found in both species are the same, the study reported a doubly charged ion with an *m/z* of 973.59 (z=-2) to be present only in *B. pseudomallei*. These results and the potential influence of lipid A on virality of bacterial species indicate the need for further structural characterization of lipid A in *B. pseudomallei* and *B. thailandensis*.

1.2 Mass Spectrometry

Mass spectrometry is an analytical technique in which different molecules are analyzed according to their mass-to-charge (*m/z*) ratios. IUPAC defined mass spectrometry as "the study of matter through the formation of gas-phase ions that are characterized using mass spectrometers by their mass, charge, structure and/or physico-chemical properties."[22] A mass spectrometer is an instrument that measures the mass of analyte molecules in an ionized state. J. J. Thomson, the father of mass spectrometry, was the first person to use a mass spectrometer and by doing so he discovered the electron and measured its *m/z*.[23]

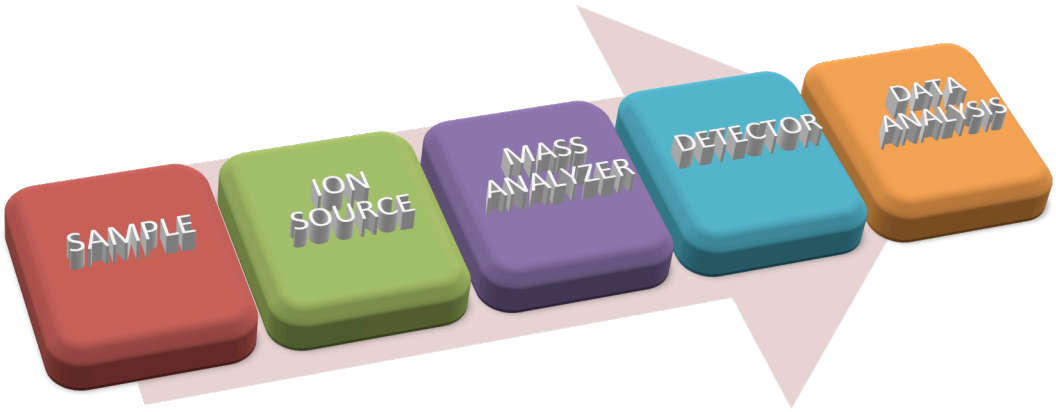

Figure 1-1: Schematic of a mass spectrometer

A schematic of a mass spectrometer is shown in Figure 1-1. The different processes in a mass spectrometer are:

1. Formation of ions and their transformation into gas phase, which happens in the ionization source
2. Separation of these gas-phase ions based on their mass-to-charge (*m/z*) ratios in the mass analyzer
3. Fragmentation of ions, and the analysis of their fragments in a second mass analyzer
4. Detection of ions coming from the last analyzer and measurement of their abundance with a detector that converts the ions into electrical signals
5. Transmission of the signals from the detector to the computer

The different ionization sources that are being commonly used in a mass spectrometer are: electron ionization (EI), chemical ionization (CI), ESI, MALDI and inductively coupled plasma (ICP).[24] Over the years, various mass analyzers were developed to separate ions according to their *m/z* values in a mass spectrometer. Among the various mass analyzers, frequently used are the quadrupole, time-of-flight (TOF), ion trap, magnetic sector, orbitrap, or a combination of these. The detectors typically used in a mass spectrometer are an electron multiplier or microchannel plates.[24]

1.2.1 Matrix-Assisted Laser Desorption/Ionization Mass Spectrometry (MALDI-MS)

Traditional mass spectrometric instruments were used to analyze molecules with low molecular weights. To analyze high molecular weight compounds, it is deemed necessary to convert the molecules in condensed phase into ions in gas phase. It was difficult to perform this process, as many biopolymers are polar in nature with high molecular masses. Various new ionization techniques have been developed to overcome this problem, such as: field desorption, plasma desorption, ESI and laser desorption (LD). ESI and LD are the most widely used techniques for the analysis of biomolecules.

Lasers have been used in mass spectrometry since the early 1960s, to generate ions for the analysis of different biomolecules in mass spectrometers.[25] Transfer of energy to the sample when it absorbs energy at a specific wavelength of the laser is considered as the general principle responsible for generating ions using lasers. The main drawback of LD is its limitation in usage for high molecular weight molecules. Tanaka et al.[26] as well

as Hillenkamp and Karas[25] discovered the solution to the problem by using nanoparticle and organic molecule matrices for LDI-MS analyses involving high mass molecules.

This new technique was named matrix - assisted laser desorption/ionization mass spectrometry (MALDI-MS).[25] As the name suggests, analyte is mixed with a saturated solution of the matrix and analyzed using MALDI-MS. MALDI-MS is a soft ionization technique where laser-induced desorption results in the formation of a large number of analyte ions that are measured with high mass accuracy and high sensitivity. Mass spectrometers with different combinations of lasers like ultraviolet (UV) and infrared (IR) are used, with UV being the most widely used laser.[25] Common lasers used in MALDI are listed in Table 1-1.[24]

Table 1-1: Different Types of Lasers Used in MALDI-MS and Their Wavelengths

LASER	WAVELENGTH
Nitrogen	337 nm
Nd:YAG	266 nm or 355 nm
Er:YAG	2.94 μm
Carbon dioxide	10.6 μm

The general principle of MALDI-MS is shown in Figure 1-2. Sample preparation involves co-crystallization of the sample with a matrix. The matrix along with the analyte is then subjected to laser irradiation. The photons from the laser cause desorption and ionization of both the matrix and the sample in the gas phase. These ions are then accelerated through a drift tube where they are separated according to their speed.

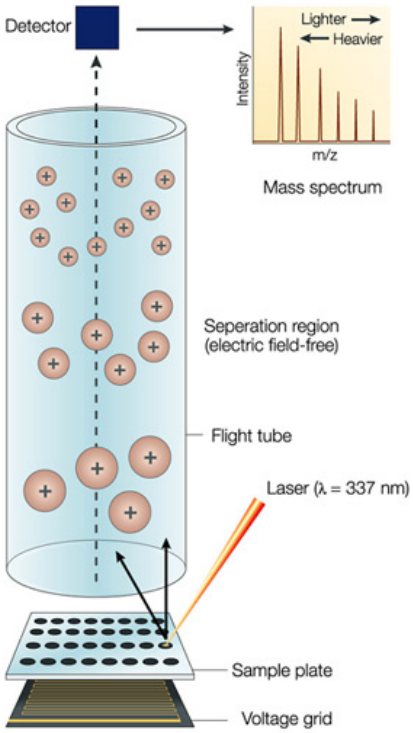

Figure 1-2: Principle of MALDI-TOF MS.[27] Reprinted with permission from reference 27.

The speed with which the ions move in the drift tube depends on its *m/z*. Ions with a high mass-to-charge ratio move slowly in the drift tube and ions with a low mass-to-charge ratio move with a higher speed. Hence, smaller ions reach the detector first and larger ions reach the detector more slowly. This is given by the equation 1-1:[28]

$$m/z = 2eU\,(t*L^{-1})^2 \quad \text{(eq. 1-1)}$$

In the above equation, m stands for mass, z for charge state, e for elementary charge, U for potential difference, t for time-of-flight to the detector, and L for the length of the drift tube.

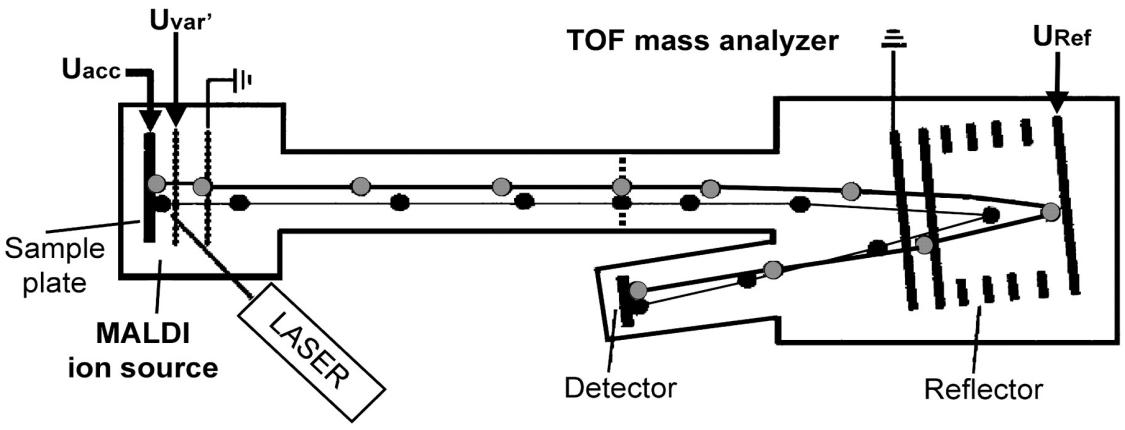

Figure 1-3: Schematic of MALDI-MS.[29] Reprinted with permission from reference 29.

The mass analyzer used in MALDI is known as time-of-flight (TOF) as the mass is determined by the time the ion is in the drift tube. A schematic of MALDI-MS with the TOF mass analyzer is shown in Figure 1-3. The MALDI-MS instrument used in this study has two mass analyzers, a linear TOF and a reflectron TOF. A reflectron typically increases the time-of-flight of an ion in the drift tube. Use of reflectron TOF results in an increase in the mass resolution as the ion spends more time in the drift tube.[28]

Selection of a suitable matrix is of primary importance as it enhances ion formation by photoexcitation or photoionization of the matrix molecules.[28] The analyte is co-crystallized with saturated matrix solution and, upon laser irradiation, the matrix is vaporized along with the analyte.

The matrix can act as both proton donor and proton acceptor,[30] and hence can help ionization of the analyte molecules both in positive ion mode and negative ion

mode, respectively. Different matrices are used for analyzing different classes of molecules. The most commonly used matrices are provided in Table 1-2.[24, 28]

Table 1-2. Type of Matrices Used for Different Types of Biomolecules in MALDI-MS

ANALYTE	MATRIX
Peptides/Proteins	α-Cyano-4-hydroxycinnamic acid (CHCA), 2,5-Dihydroxybenzoic acid (DHB), Sinapic acid (SA)
Oligonucleotides	Trihydroxyacetophenone (THAP), 3-Hydroxypicolinic acid (HPA)
Carbohydrates	α-Cyano-4-hydroxycinnamic acid (CHCA), 2,5-Dihydroxybenzoic acid (DHB), Trihydroxyacetophenone (THAP)
Lipids	Dithranol (DIT), 2,5-Dihydroxybenzoic acid (DHB)

1.2.2 Electrospray Ionization Mass Spectrometry (ESI-MS)

In 1989, John Fenn, introduced a new method of ionization known as ESI, which is a soft ionization technique and ionizes proteins by multiple charging.[31] Development of ESI and MALDI solved the problem of structural destruction of analyte molecules by different ionization methods. The major advantage of ESI is that it forms ions with multiple charges. Multiple charging lowers the *m/z* of the ions formed, allowing them to fall in a mass range suitable for all common mass analyzers. ESI has become a powerful

tool for the analyses of large biomolecules like proteins and nucleic acids. Applications of ESI are not limited to biological molecules and proteomics, but are spread out to a range of analytes like polar organic molecules[32], inorganic molecules[33] and metal-organic complexes.[34]

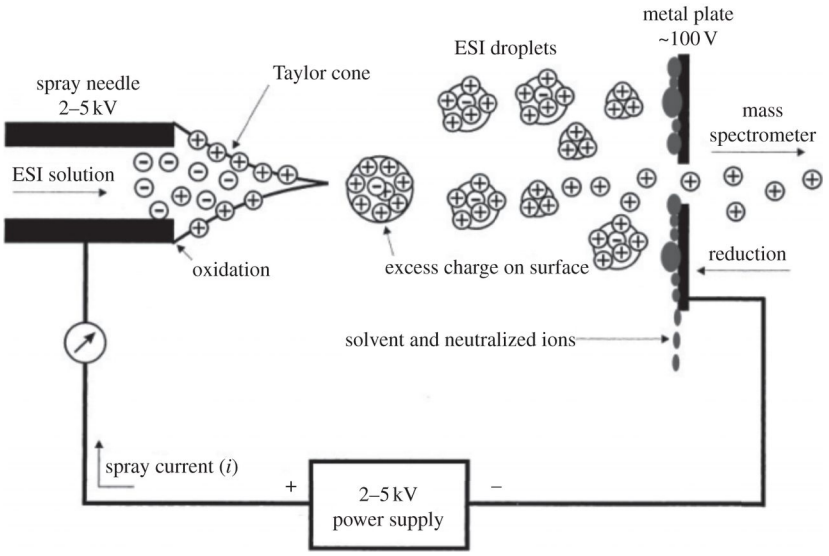

Figure 1-4: Principle of ESI-MS.[35] Reprinted with permission from reference 35.

The principle of ESI-MS is shown in Figure 1-4. ESI-MS is composed of an ion source, mass analyzer and detector. The ions are formed at atmospheric pressure in the ionization chamber, and are then transferred to the mass analyzer via ion optics-like skimmer, focusing lens, multipole, etc., which help maintain a stable trajectory of the ions. The role of the mass analyzer is to separate the ions based on their *m/z* values before the ions are further passed to the detector. All of these processes are conducted under a high vacuum, typically 10^{-3} torr to 10^{-6} torr, as the gas-phase ions are short-lived and highly reactive.[36]

A very low concentration of the analyte solution is injected into the mass spectrometer by a syringe pump through a stainless steel capillary. The flow rate is

typically between 1-10 μL/min. A voltage of 2-6 kV is applied to the tip of the capillary that results in the formation of an electric field. The electric field will be the highest at the tip of the capillary. The effect of the electric field increases as the voltage is increased.[36] At low voltages, the droplets formed at the tip of the capillary are spherical. As the charges accumulate at the tip, the droplets elongate and when the surface tension is broken, the shape of the droplets changes to a cone. This cone is known as a Taylor cone.[37] An aerosol of electrospray droplets of the sample solution is formed due to the high electric filed. The flow of N_2 gas around the capillary improves nebulization and also helps in directing the spray of ions towards the mass spectrometer. Solvent evaporation causes the charged droplets to decrease in size, which is supported by the flow of nitrogen (drying gas).

Different types of mass analyzers are used in ESI-MS such as magnetic (B)/ electric (E) sector, linear quadrupole ion trap (LIT), three-dimensional quadrupole ion trap (QIT), orbitrap, TOF, and ion cyclotron resonance (ICR).[24, 38-39]

The most commonly used detector in ESI-MS is the electron multiplier. In this type of detector, the ions strike a metal or a semiconductor plate called a dynode, which emits secondary electrons.[24] The secondary electrons are accelerated towards the second and subsequent dynodes. The electrons emitted are increased at each dynode. There are several types of electron multipliers such as channel electron multipliers (CEMs) or microchannel plates (MCPs).[38]

1.2.2.1 Mechanisms of ion formation in ESI:

Two mechanisms have been proposed to explain the process of gas-phase ion formation in ESI: charge residue model (CRM) and ion evaporation model (IEM).[36]

Charge Residue Model*:* Dole proposed this model in 1968.[40, 41] This mechanism is called the charge residue model because the analyte retains a charge in the gas phase during the ES process. The mechanism proceeds as follows:

An extremely small charged droplet is formed due to solvent evaporation and coulombic explosion, which contains only one analyte molecule. Desolvation of this droplet causes the charge to retain on the analyte. The repulsion of charges tends to increase until the droplet reaches the Rayleigh stability limit.

Rayleigh stability limit is given by the following equation 1-2:

$$q = 8\pi (\varepsilon \gamma R^3)^{1/2} \quad \text{(eq. 1-2)}$$

In the above equation, q is the charge, ε is the electrical permittivity of the surrounding medium, γ is the surface tension of the solvent, and R is the radius of the droplet.

Ion Evaporation Model: Iribarne and Thomson proposed this mechanism.[37, 42] Due to repeated solvent evaporation and coulombic explosion, the radii of the charged droplets decrease to a given size. When the radii of the droplets reach the size $R \leq 10$ nm, direct emission of the solvated ions is possible.

Major advantages of ESI-MS are:

a. Ability to form and detect multiply charged ions of the analyte
b. High sensitivity
c. Ability to measure high molecular weight analytes

1.3 Lipopolysaccharide (LPS)

Various amphiphilic macromolecules are found to be present on the outer membrane of a Gram-negative bacterium. LPSs are considered to be one of these macromolecules with exceptional significance that are seen on the outer membrane of bacteria.[13] LPSs are amphiphilic molecules[7], which are bound to the Gram-negative bacterium by a hydrophobic anchor known as lipid A.[11] LPSs are involved in regular membrane functions, but also have a unique job related to immune response. By stimulating the formation of antibodies, LPSs are involved in the recognition of host's defense system during infection.[43]

General structure of a LPS is shown in Figure 1-5. LPSs contain three structural components, which are covalently bound to each other: (i) a long "O-specific polysaccharide" (OPS) consisting of repeating units of monosaccharide′s (typically from one to seven) that are responsible for O-antigenic specificity, (ii) a core oligosaccharide region (core OS), which is subdivided into an inner core and outer core, and (iii) a hydrophobic region termed as "lipid A" that anchors the LPS to the outer membrane of Gram-negative bacteria by hydrophobic interactions.[13]

These LPSs are further divided into three types based on their structural components.[13] A smooth (S-type) LPS consists of all three domains, which are common in wild-type strains of bacteria. These are also known as long chain LPSs. A semi-rough (SR-type) LPS (also called a short chain LPS) has only one O-chain repeating unit attached to the core oligosaccharide. Rough (R-type) LPSs are completely devoid of the O-specific polysaccharide chain due to genetic defects.[44] The endotoxic activity of S-type LPS and R-type LPS were compared and it is indicated that the endotoxic activity is due to the lipid A moiety.[13]

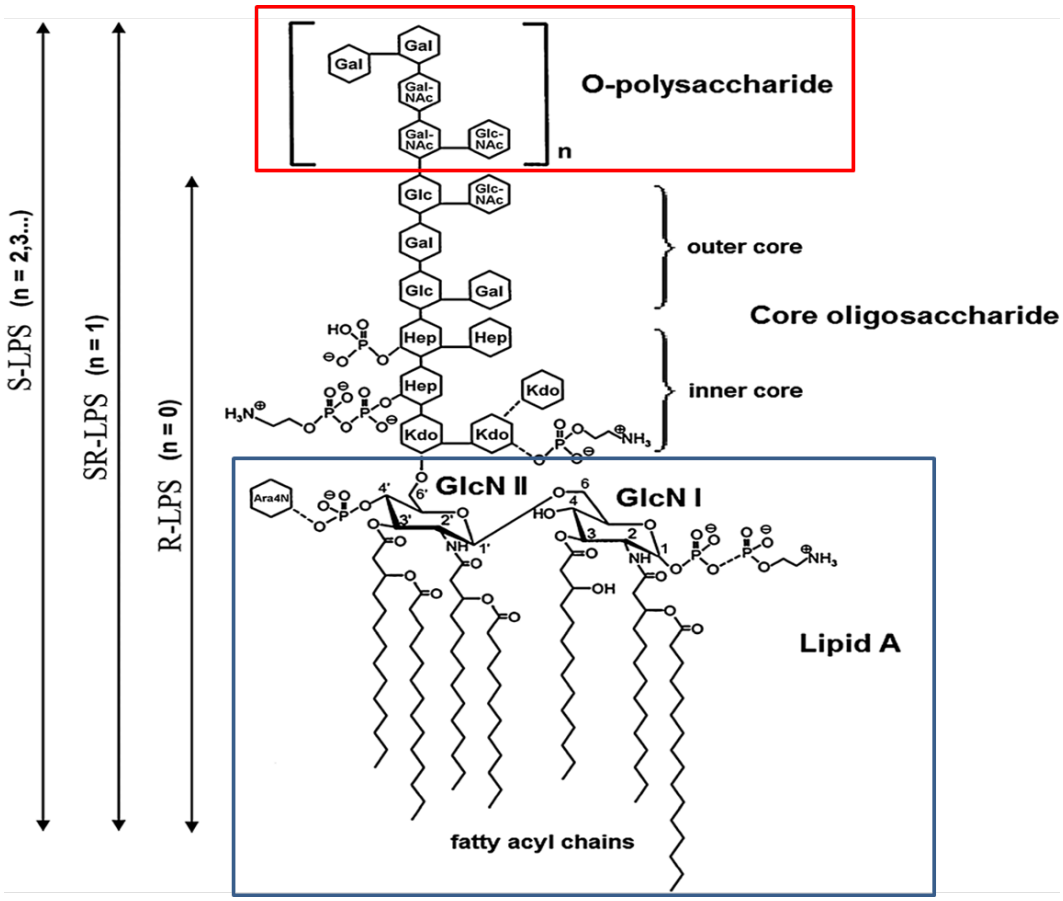

Figure 1-5: General structure of a LPS.[6] Reprinted with permission from reference 6.

The three major components of a LPS are O-antigenic region, core region, and lipid A portion. The O-specific antigen has high structural variability[45] consisting of repeating oligosaccharide units. Depending upon the nature, sequence, substitution, and type of linkage, the structure of these repeating units differ from strain to strain.[46]

The core oligosaccharides are structurally identical[47] and hence, show less variability. The core consists of two regions: an inner core and an outer core. The outer core is comprised of hexoses, while the inner core contains heptapyranoses and 3-deoxy-2-manno-2-octulosonic acid (Kdo). H_3PO_4 substitutes heptapyranose and Kdo. The high density of negatively charged residues has a physiological significance of concentrating the bivalent cations (Ca^{2+} and Mg^{2+}) within the cell that are required for structural and functional integrity of the outer membrane.[9, 13]

Lipid A constitutes the toxic and immunomodulating component of LPS.[48] Lipid A, a phosphoglycolipid that acts as an anchor in binding the LPS to the outer membrane has pathophysiological importance as it has intense effects when injected into a mammal. These effects include induction of endotoxin shock,[49] pyrogenecity,[50] macrophage activation,[51] interferon production,[52] and tumor regression.[53]

General structure of lipid A is shown in Figure 1-6. Lipid A is primarily composed of β-D-Glc*p*N-(1→6)-α-D-Glc*p*N disaccharide backbone, but 2,3-diamino-2,3-deoxy-glycopyranose residues are also seen in the disaccharide backbone in some bacteria.[54-55]

The disaccharide backbone is substituted with phosphoryl residues, ethanolamine phosphate, 4-amino-4-deoxy-arabinose-1-phosphate as well as with a variety of acyl chains (chain lengths are typically between 10 and 30 carbon atoms).

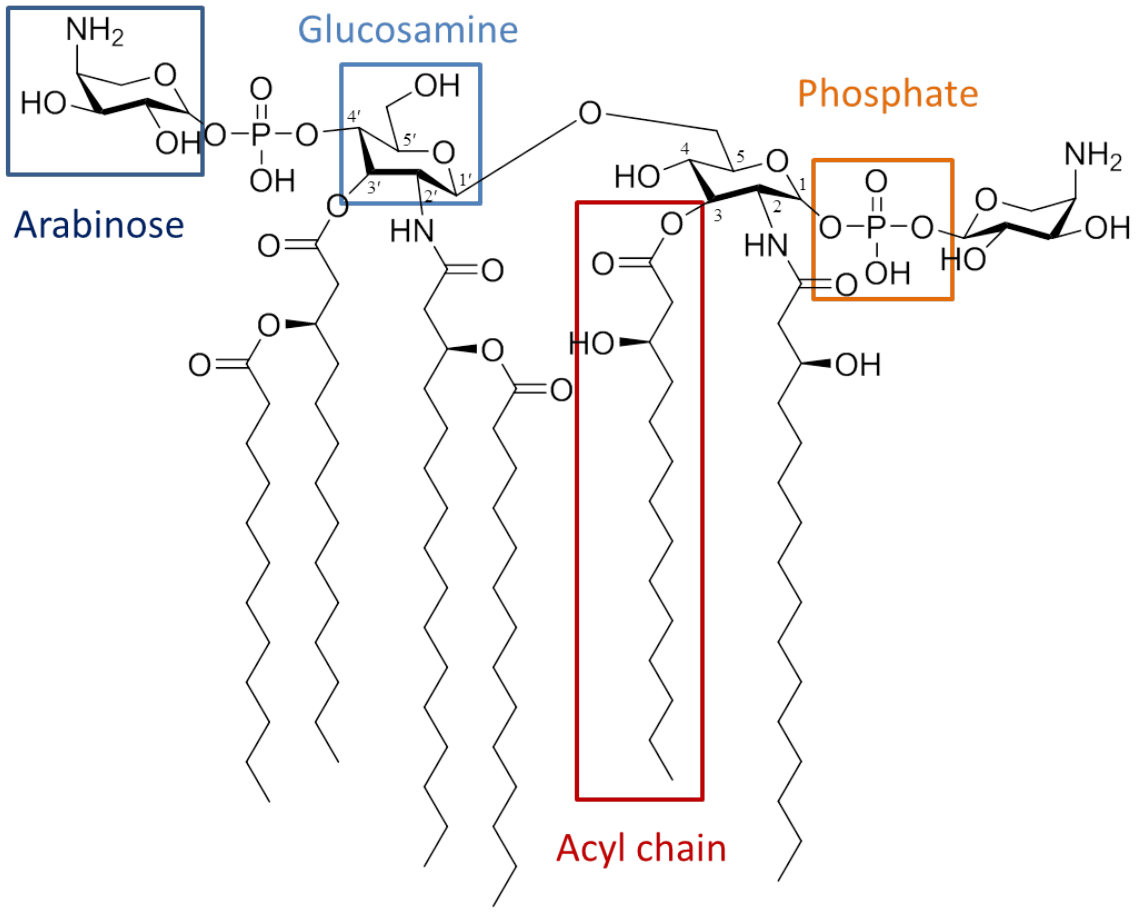

Figure 1-6: General structure of lipid A

Lipid A often contains two partially substituted phosphoryl residues.[8] One of these residues is linked to the hydroxyl group of the reducing glucosaminyl residue (GlcN I) and the other one is attached in position 4′ of the non-reducing glucosamine group (GlcN II). The carbohydrate backbone is acylated at positions 2, 3, 2′, and 3′ by four acyl chains. The acyl chains at positions 2′ and 3′ are further acylated depending on

the bacterial strain at their 3-hydroxyl group by dodecanoic acid ($C_{12:0}$), tetradecanoic acid ($C_{14:0}$) or hexadecanoic acid ($C_{16:0}$).[56-57]

Changes in acylation, phosphorylation, or glycosylation alter the endotoxic activity of the LPS in the Gram-negative bacteria.[58] Any deviation from the standard biphosphorylated hexa-acyl lipid A might lead to reduced toxicity[9] or even anti-tumor activity.[59] Phosphorylation of lipid A plays an important role in endotoxicity. The endotoxicity is reduced when a phosphate group is removed.[9, 60] Any substitutions on the phosphate group might also alter the endotoxic activity. When an arabinose sugar (Ara4N) is attached to the phosphate group, it increases the bacterial resistance to the host's cationic antimicrobial peptides.[58, 61]

1.4 MALDI-MS Analysis of Lipid A

MALDI-MS has been widely used for structural characterization of LPSs.[6, 62] One major advantage with MALDI-MS is formation of singly charged ions, which makes it easier to interpret the spectra. Due to the amphipathic nature of LPS molecules, sample preparation plays a very important role. Use of different matrices enhances the signal-to-noise ratio in the mass spectra.[63]

Schiller, et al. used MALDI-MS to study different classes of lipids including phospholipids. In this study, they tested different matrices like DHB, SA, and CHCA. Of the three matrices used, DHB gave the best results because it was shown to have better crystallization properties. [64] ATT was used as the MALDI matrix for the analysis of oligosaccharides for a long time.[65] DHB was used as a matrix for analysis of lipids and

phospholipids[66], and it is one of the mostly used matrices for the MALDI-MS analyses of lipids (Table 1.2).

Four different matrices such as ATT, DHB, THAP, and CMBT (5-chloro-2-mercaptobenzothiazole) were used by Li et al. for the analysis of lipid A from *E. coli* O116 and some other Gram-negative bacteria.[63] EDTA has also been used as a matrix additive in this study. While most ions were the same, some lipid A ions were different for each matrix. CMBT with EDTA was considered to yield the best results for studying the structures of lipid A molecules.[63]

Stübiger, et al. used ATT as a matrix for MALDI-MS analysis of oxidized phospholipids. This work confirmed that use of ATT as a matrix reduces fragmentation of intact molecules and enhances sensitivity.[67]

1.5 ESI-MS Analysis of Lipid A

ESI-MS has been in use for the analysis of lipid A for a long time.[14-15, 17, 61] Chan, et al. used ESI-MS and ESI-MS/MS for studying the structures of lipid A molecules from different strains of bacteria. A triple quadrupole instrument was used in this study. CID was performed on the lipid A samples to obtain structural information of these lipid A molecules. With CID, different groups of fragment ions were obtained, which helped in structural identification of lipid A.[18]

Kussak, et al. employed QIT-MS to identify the position of fatty acids on lipid A molecules from Gram-negative bacteria. The major advantage of an IT instrument is its ability to perform different levels of fragmentation (MS^n). Tandem mass spectrometry

experiments help in determining the degree of acylation and positions of different acyl chains. In this study, lipid A was dissolved using 1:1 chloroform/methanol and analyzed by IT-MS.[14]

Jones, et al. characterized the structure of lipid A from *Yersinia pestis* and also identified its phosphorylation patterns. An ion trap Fourier transform ion cyclotron resonance (FT-ICR) mass spectrometer was used in this study. The position of Ara4N on lipid A molecules was also identified in this study along with the position of phosphoryl groups.[68]

Novem et al. studied the lipopolysaccharides of *B. pseudomallei* KHW and *B. thailandensis* ATCC 700388 strains.[1] In this study, lipid A profiles of both bacteria were studied by using ESI-MS. A hypothetical structure (shown in Figure 1-7) was proposed based on MS and MS/MS data. In the Figure 1-7: A, B, and C depict the losses of phosphorylated arabinose, Ara4N, and HPO_3, respectively.

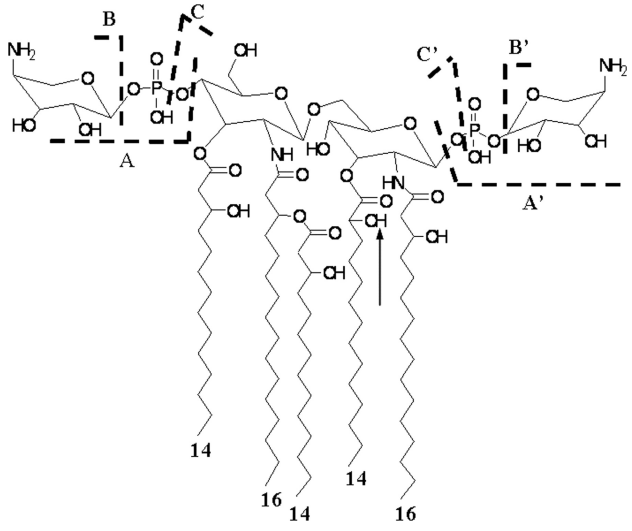

Figure 1-7: Hypothetical structure proposed by Novem et al.[1] of the major lipid A species in *B. pseudomallei*. Reprinted with permission from reference 1.

This structure explained the structures of most lipid A ions observed in ESI-MS spectra. This study hypothesized that a difference of 2-OH (shown with an arrow in Figure 1-7) on $C_{14:0}$ acyl chain at position 3 was observed between the lipid A structures of *B. pseudomallei* and *B. thailandensis*.[1] Detection of this modification is believed to lead to a doubly charged ion with an *m/z* value of 973.59 found only in *B. pseudomallei* lipid A. Considering that this structure is hypothetical, further studies of *Burkholderia* lipid A are needed.

Chapter 2

Materials and Methods

2.1 Isolation of Lipid A

2.1.1 Materials for Lipid A Isolation

B. pseudomallei (strain 1026b), *B. thailandensis* (strain E264), flasks**,** Luria Broth (LB) media, proteinase K, RNase, DNase, phenol, milli-Q-DI H_2O, 70 mL UC polybottles, 12 mL-capacity slide-A-lyzer dialysis cassettes with 7 kDa molecular weight cutoff were provided in the laboratory of Dr. R. Mark Wooten at the University of Toledo College of Medicine and Life Sciences.

2.1.2 Lipopolysaccharide and Lipid A Isolation Protocol

Bacterial strains were grown in a biosafety level 3 facility at the University of Toledo College of Medicine and Life Sciences by trained personnel (Dr. Michael Bechill) following the safety guidelines and previously published protocols for lipid A isolation.[69-73] The bacteria were cultured on a low salt LB (Luria Broth) agar plate which was

maintained at 37 °C overnight. 500 mL of LB media was inoculated with $1x10^6$ bacteria per milliliter in a 1 L beveled flask and incubated at 37 °C at 200 rpm until the bacteria were at mid-log phase. This took approximately 10 h. 40 mL aliquots of the bacteria were then aliquoted into 50 mL tubes and centrifuged. The supernatant was discarded. The above steps were repeated until all 500 mL of LB media was pelleted. The pellets were washed twice with phosphate buffered saline (PBS) and centrifuged at 14,000 x *g* for 5 min. The bacteria were suspended in 25 mL of 90% phenol at 68 °C.

Hot phenol-water extraction was performed. The lysate obtained in the previous step was placed in a heat block at 68 °C. 25 mL of Milli-Q-DI H_2O was added to the lysate and transferred to a 50 mL BD Falcone tube. The tube was placed in the 68 °C heat block and vortexed for 20 min intermittently. The aqueous phase was collected once the lysate was cooled to room temperature. 12 mL of the aqueous phase was injected into two 7 kDa MW Slide-A-Lyzer dialysis cassettes. The aqueous phase was dialyzed against Milli-Q-DI H_2O (~1800 mL per change for 5 changes in a 2 L beaker) to remove residual phenol. The initial wash was disposed of as hazardous waste and remainder of the washes were disposed of in the municipal waste stream. Insoluble cell debris was pelleted at 14,000 x *g* for 5 min. The supernatant was lyophilized to be concentrated. The lyophilizer collection chamber was cleaned with 70% ethanol (EtOH) and rinsed with Milli-Q-DI H_2O. The lyophilizer was turned on and set to cool to a temperature of -50 °C. Once cooled, the pump was turned on and the lyophilizer was allowed to reach vacuum and was equilibrated for 30-60 min.

All of the aqueous phase from previous step was added to a wide mouth freeze dry flask and covered with plastic wrap. The sample was placed in a -50 °C freezer at a

45° angle until completely frozen. The sample was then placed in dry ice once it was completely frozen and it was lyophilized. The lyophilized sample was transferred to a 50 mL BD Falcone tube. The crude carbohydrate portion preparation was solubilized at a concentration of ~30 mg/mL in 100 mM Tris-HCl. To the above portion, RNase (50 μg/mL) and DNase (50 μg/mL) were added and the sample was left at 37 °C overnight. Then proteinase L (100 μg/mL) was added to the sample and the sample was incubated at 65 °C for 1 h. The lysate was ultra-centrifuged to obtain a gel-like pellet of LPS. The pellet of LPS was then resuspended in 40 mL of limulus amebocyte lysate (LAL) reagent water and transferred to a 15 mL conical tube to lyophilize and concentrate the purified LPS.

Lipid A was separated from LPS by suspending 0.5 mg of lyophilized LPS in 100 μL of 0.01M TEA citrate and vortexing vigorously. The suspension was sonicated 4 times for 30 s each. The sample was incubated at 100 °C for 2 h vortexing every 15 minutes for 30 s. The final lipid A samples were stored at 4 °C in a refrigerator until needed.

2.2. O-deacylation of Lipid A (Partial and Complete O-deacylation)

The lipid A samples were subjected to deacylation protocol using ammonium hydroxide and methylamine (Sigma). For partial O-deacylation, the lipid A sample was dissolved in 28% of ammonium hydroxide (NH_4OH) solution[74] to a concentration of 1 mg/mL and then stirred for 5 h at 55 ^{o}C. Complete O-deacylation of the lipid A sample was achieved by using a 41% methylamine (CH_3NH_2) solution.[75] The sample was

dissolved in the methylamine solution and stirred for 5 h at 37 ^{o}C. Both sample solutions were then evaporated using a vacuum concentrator and resuspended in 2:3:2 chloroform: methanol: water (v/v/v).

2.3 Mass Spectrometry of Lipid A

2.3.1 Materials

HPLC-grade methanol and water, and ACS-grade chloroform were purchased from Fisher Scientific. Matrices ATT, DHB, and THAP were purchased from Sigma.

2.3.2 MS Experiments

Purified lipid A samples were further extracted using a mixture of chloroform, methanol, and water (2:3:2; v: v: v). ~ 0.5 mg of lyophilized lipid A sample was dissolved in 0.5 mL of chloroform, methanol, and water (2:3:2; v: v: v) mixture. Samples were then vortexed and allowed to sit until there was a clear separation into two immiscible layers. Lipid A for MS analyses was taken from chloroform/methanol (bottom) layer. MALDI-MS instrument UltrafleXtreme (Bruker) and ATT matrix were used for MALDI-MS analyses. 1 μL of the sample solution was mixed with 1 μL of matrix solution and deposited onto a MALDI plate.

For ESI-MS, lipid A was extracted using the solvents mentioned above. Chloroform/methanol layer (bottom layer) was injected into the ESI source of the mass spectrometer at the flow rate of 1.5 μL/min using a syringe pump. MS, MS/MS, and MS/MS/MS spectra were obtained in mass spectrometry facility at Fred Hutchison

Cancer Research Center (FHCRC, Seattle, WA) using an Orbitrap Elite (Thermo) mass spectrometer. Also, Waters Q-TOF-ESI-MS was used to obtain both MS and MS/MS data. The source temperature was 80 °C, desolvation temperature was 120 °C, capillary was maintained at a voltage of 2.4 kV, and the sample cone was 30 V. Additionally, MS and MS/MS experiments were also performed on Orbitrap Fusion (Thermo). A spray voltage of 2.2 kV was used. For MS/MS collision energy of 35 V was used.

Chapter 3

Results

3.1. MALDI-MS and MALDI-MS/MS Analyses of Lipid A from *B. pseudomallei* Strain 1026b and *B. thailandensis* Strain E264

Lipid A was successfully isolated from *B. pseudomallei* strain 1026b and *B. thailandensis* strain E264 using the hot phenol-water extraction method. Liquid-liquid extraction of lipid A in chloroform, water and methanol was performed immediately before MS analyses of lipid A. Matrices like ATT, DHB, and THAP were tested for MALDI-MS analyses of lipid A, but ATT was chosen as the matrix for further MALDI-MS analyses as it gave better spectra with higher intensities of the ions than DHB and THAP. MALDI-MS spectrum of *B. pseudomallei* 1026b lipid A in negative ion mode (Figure 3-1) using ATT as matrix shows intense peaks at *m/z* values of 1363.988, 1443.968, 1495.023, 1580.040, 1670.135, 1722.138, and 1801.231 that correspond to deprotonated lipid A molecules. The lipid A ions were assigned using a hypothetical

structure (M=2113.383) shown in the inset of Figure 3-1, which was derived by addition of a $C_{12:1}$ (M=182.159) acyl chain to a hypothetical structure (M=1933.231) proposed by Novem et al.[1] Since an ion with an *m/z* value of 1580.040 was observed, but could not be explained by the proposed structure by Novem et al. (Figure 1-7), a new hypothetical structure was proposed.[1] When compared with the hypothetical structure proposed by Novem et al.[1] (Figure 1-7) the main difference is a $C_{12:1}$ acyl chain attached to the 3-hydroxyl group on the ester linked acyl chain ($C_{14:0}$) and a 2-hydroxy tetradecanoic acid $C_{14:0}$(2-OH) acyl chain located at position 3 on the disaccharide backbone. This ester linked acyl chain is located at position 3′ on the sugar backbone. The primary reason for proposing a new hypothetical structure was to structurally characterize the lipid A species with an *m/z* value of 1580.040 as this lipid A species was believed to be the main difference between lipid A species from *B. pseudomallei* 1026b and *B. thailandensis* E264.

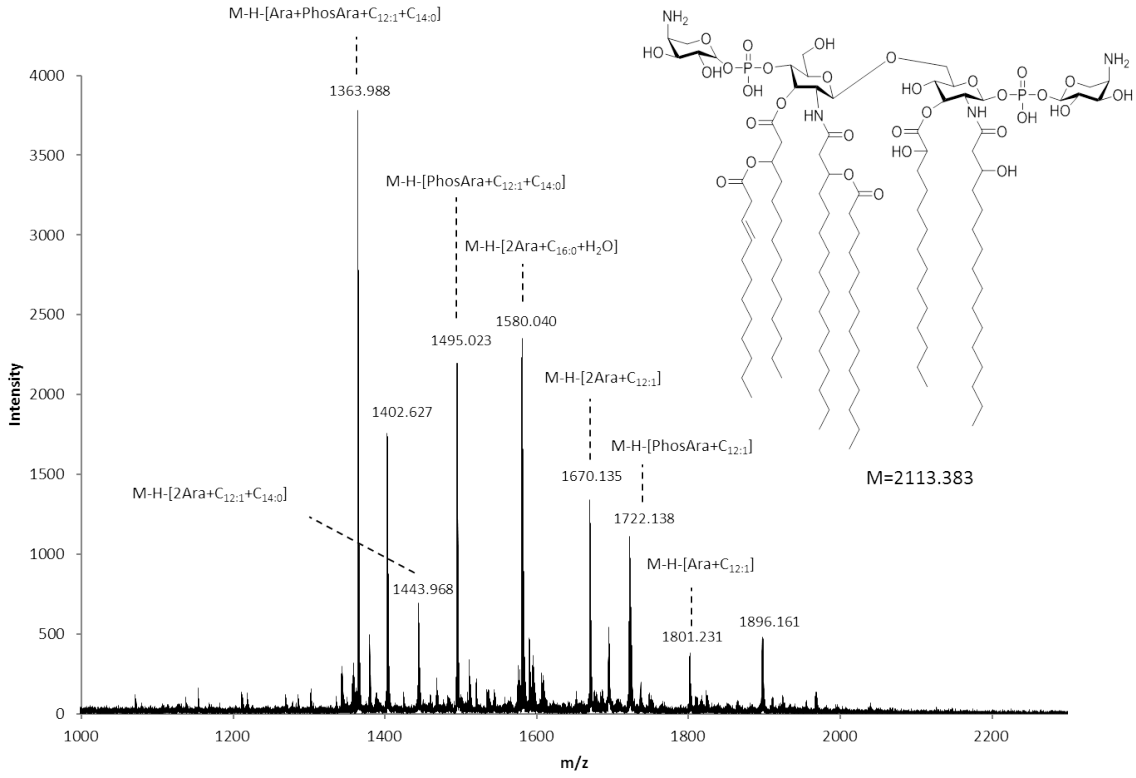

Figure 3-1: A MALDI-MS spectrum of lipid A from *B. pseudomallei* 1026b acquired in negative ion mode using ATT as the matrix. Inset: hypothetical structure of the parent lipid A molecule.

In the MALDI-MS spectrum of lipid A from *B. pseudomallei* 1026b shown in Figure 3-1, the ion with an *m/z* of 1801.231 can be formed by the loss of a secondary $C_{12:1}$ acyl chain located on the $C_{14:0}$ acyl chain at position 3′ and an Ara4N attached to the phosphate at position 1 on the sugar backbone of the parent structure. Loss of another Ara4N attached to the H_3PO_4 at position 4 results in an ion with an *m/z* of 1670.135. Loss of PO_3^-, from the ion with an *m/z* of 1801.231, gives the ion with an *m/z* value of 1722.138. Further loss of a primary $C_{14:0}$ acyl chain at position 3′, results in formation of

an ion with an *m/z* value of 1495.023. Similarly, the ion with an *m/z* of 1443.968 is due to loss of the primary ester linked $C_{14:0}$ acyl chain, at position 3, from the ion with an *m/z* value of 1670.135. Additional loss of HPO_3 at position 4 on the disaccharide backbone results in formation of an ion with an *m/z* value of 1363.988.

The MALDI-MS spectrum of the lipid A species from *B. thailandensis* E264 obtained in negative ion mode (Figure 3-2) contains many of the same deprotonated lipid A species (e.g., *m/z* values of 1364.862, 1443.824, 1494.908, 1670.027, 1722.102, and 1801.076) as the MALDI-MS spectrum of *B. pseudomallei* 1026b, but the ion with an *m/z* of 1580.040 is unique for lipid A originating from *B. pseudomallei* 1026b (Table 3-1). Ions with *m/z* values of 1402.627, 1896.161, 1967.289, and 2039.259 (Table 3-1) were also unique for lipid A from *B. pseudomallei* 1026b, but their intensities were inconsistent and relatively low.

In the MALDI-MS spectrum of *B. thailandensis* E264 lipid A, the ion with an *m/z* of 1801.076 is due to loss of an Ara4N attached to the phosphate group at position 1 of the disaccharide backbone from the parent lipid A molecule (shown in the inset of figure 3-2).[1] Loss of PO_3^- located at position 1 from this lipid A ion with an *m/z* of 1801.076, results in formation of an ion with an *m/z* of 1722.102. Loss of Ara4N attached to the phosphate located at position 4′ from lipid A ion with an *m/z* of 1722.102 forms an ion with an *m/z* value of 1590.048. The ion with an *m/z* value of 1443.824 is due to loss of two Ara4N moieties and a $C_{14:0}$ acyl chain from the parent molecule. Loss of another HPO_3 results in the formation of an ion with an *m/z* of 1364.862. All intense ions mentioned above, except the ion with an *m/z* of 1580.040, can be deduced from the

hypothetical structure of *B. pseudomallei* lipid A (*m/z* of deprotonated molecule ~ 1932.20) proposed by Novem et al.[1] (Inset of Figure 3-2).

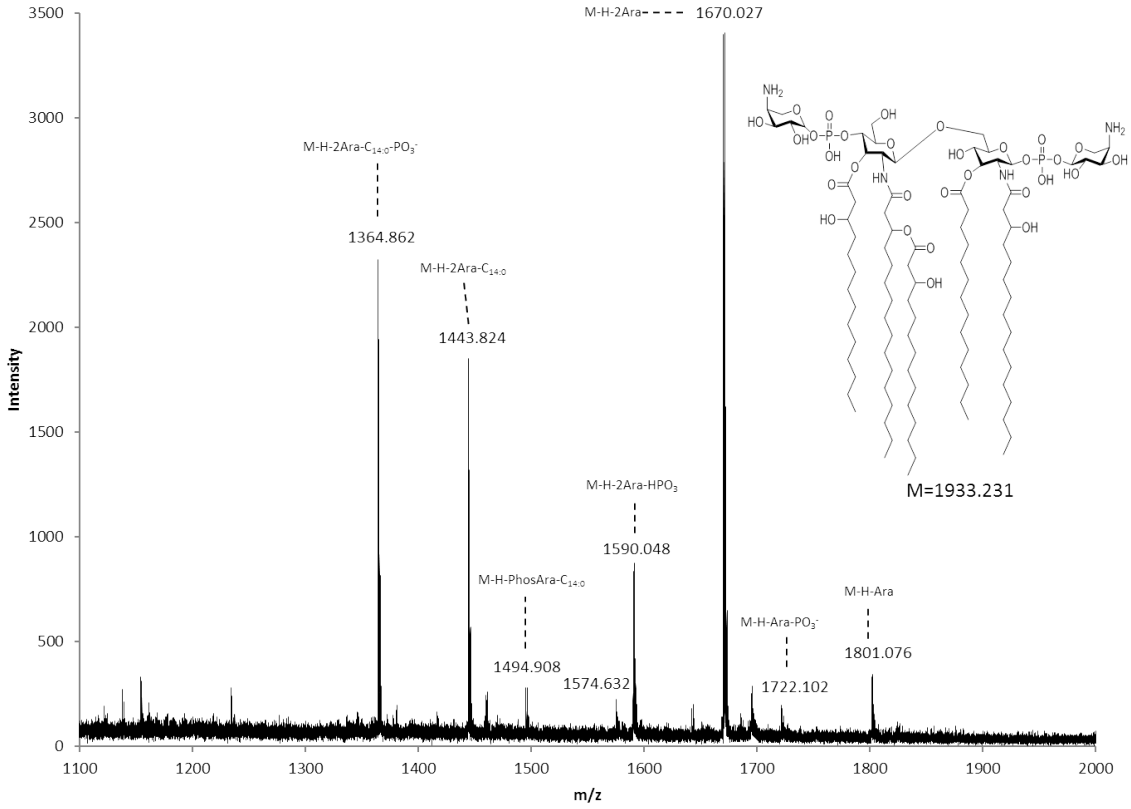

Figure 3-2: A MALDI-MS spectrum of lipid A species from *B. thailandensis* E264 in negative ion mode using ATT as the matrix. Inset: hypothetical structure of the parent lipid A molecule proposed by Novem et al.[1]

The acyl chain that is present at position 3 on the disaccharide backbone is a ($C_{14:0}$), which in the case of our proposed lipid A structure from *B. pseudomallei* 1026b is a $C_{14:0}$(2-OH).[1, 4]

While the lipid A ion with an *m/z* of ~1932 was not observed in our mass spectra,[1] the ions detected were derived from the structure proposed by Novem et al.[1] if one considers the neutral losses of Ara4N residues, phosphoric acid and acyl chains, as well as, their losses upon fragmentation from the lipid A structures. For example, the ion with an *m/z* of 1801.231 is due to neutral loss of an Ara4N (M=~131) from the lipid A structure with an *m/z* of ~1932. An additional loss of PO_3^- will yield the ion with an *m/z* of 1722.138. The ion with an *m/z* of 1670.135 is due to loss of an Ara4N from the ion with an *m/z* of 1801.231. Loss of phosphorylated Ara4N along with a $C_{14:0}$ acyl chain from the parent lipid A molecule gives rise to an ion with an *m/z* of 1495.023. Additional loss of another Ara4N from this ion results in an ion with an *m/z* of 1363.988. The lipid A ion with an *m/z* value of 1443.968 is due to loss of two Ara4N molecules, $C_{12:0}$, and $C_{14:0}$ from the parent lipid A ion. Loss of HPO_3 from the lipid A ion with an *m/z* of 1443.968 results in the formation of lipid A ion with an *m/z* value of 1363.988. However, as mentioned above, an intense ion with an *m/z* of 1580.040 could not be assigned using the structure described by Novem et al.[1]

However, all ions can be described by using a hypothetical lipid A structure with (M= ~2113), which is shown in the inset of Figure 3-1. If this structure is considered, the ion with an *m/z* of 1580.040 would be a pentaacylated structure including two phosphoryl residues (Figure 3-7, inset). MALDI-MS/MS data yielded additional information about structures of lipid A ions confirming the assignments mentioned above.

Table 3.1: Experimental and Theoretical Masses of Each Lipid A Ion from *B. thailandensis* and *B. pseudomallei* Along with Their Composition

Exp mass (BTLA)	Exp mass (BPLA)	Ion (*m/z*) from ChemBioDraw	Acyl chains, phosphates and arabinoses
1363.882*[X]	1363.998*[X]	1363.955	Two $C_{16:0}$(3-OH), $C_{14:0}$(3-OH), $C_{14:0}$, one phosphate
1443.824*[X]	1443.968*[X]	1443.922	Two $C_{16:0}$(3-OH), $C_{14:0}$(3-OH), $C_{14:0}$, two phosphates
1494.908*	1495.023*	1495.014	Two $C_{16:0}$(3-OH), one $C_{14:0}$(3-OH), $C_{14:0}$, one phosphate, one Ara4N
-	1580.040	1580.047	Two $C_{14:0}$, one $C_{14:0}$(3-OH) with secondary $C_{12:1}$, one $C_{16:0}$(3-OH), two phosphates
1590.048*	1590.212*	1590.149	Two $C_{16:0}$(3-OH), two $C_{14:0}$(3-OH), $C_{14:0}$, one phosphate
1670.027*[X]	1670.135*[X]	1670.115	Two $C_{16:0}$(3-OH), two $C_{14:0}$(3-OH), $C_{14:0}$, two phosphates
1722.102*	1722.138*	1722.207	Two $C_{16:0}$(3-OH), two $C_{14:0}$(3-OH), $C_{14:0}$, one phosphates, one Ara4N
1801.076*[X]	1801.231*[X]	1801.173	Two $C_{16:0}$(3-OH), two $C_{14:0}$(3-OH), $C_{14:0}$, two phosphates, one Ara4N

*** - based on Novem′s structures. X – based on deacylation studies and MS/MS. Ions with an *m/z* of 1402.627, 1896.161, 1967.289, and 2039.259 were seen only in lipid A from *B. pseudomallei.***

.

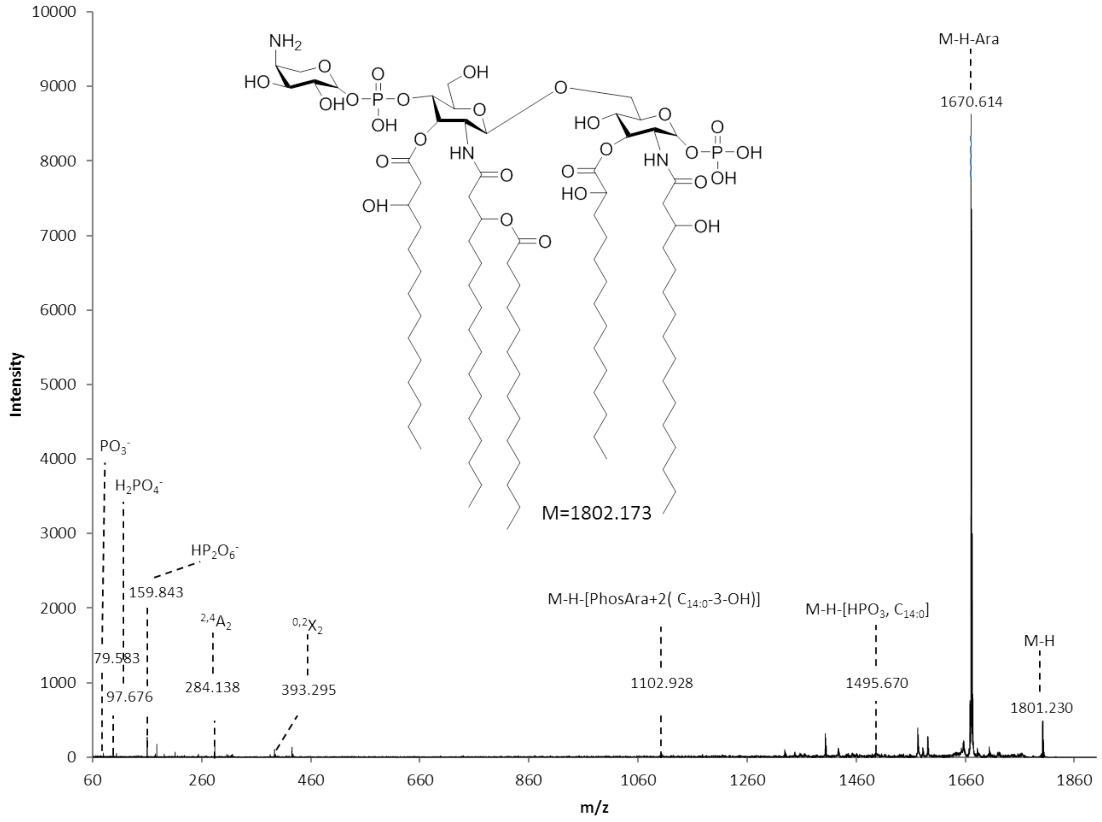

Figure 3-3: A MALDI-MS/MS spectrum of the ion with an *m/z* of 1801.231 of lipid A from *B. pseudomallei* 1026b in negative ion mode using ATT as the matrix. Inset: hypothetical structure of the parent lipid A molecule

For example, MS/MS of the parent ion with an *m/z* of 1801.231 (Figure 3-3) reveals the presence of two ions with an *m/z* of 1670.614 and 1495.670, which were also observed in the MS spectrum of *B. pseudomallei* lipid A (Figure 3-1). The ion with an *m/z* of 1670.614 is due to loss of an Ara4N group and the ion with an *m/z* of 1495.670 is due to loss of HPO_3 and a $C_{14:0}$ acyl chain. The ion with an *m/z* of 1102.928 arises due to loss of a phosphorylated Ara4N and two $C_{14:0}$ acyl chains. Two cross-ring fragments were also observed in the spectrum: ions with *m/z* values of 393.295 ($^{2,4}A_2$) and 284.138

($^{0,2}X_2$). The cross-ring fragments were assigned according to Domon and Costello's nomenclature of carbohydrate fragmentation.[76] The peak at an *m/z* value of 244.240 confirms the presence of $C_{14:0}$(3-OH). The presence of phosphoryl residues was confirmed by the presence of ions with *m/z* values of 79.583 (PO_3^-), 97.676 ($H_2PO_4^-$), 159.843 ($HP_2O_6^-$), and 177.830 ($H_3P_2O_7^-$).

From the MS/MS data of the ion with an *m/z* of 1670.135, fragments are assigned as shown in Figure 3-4.

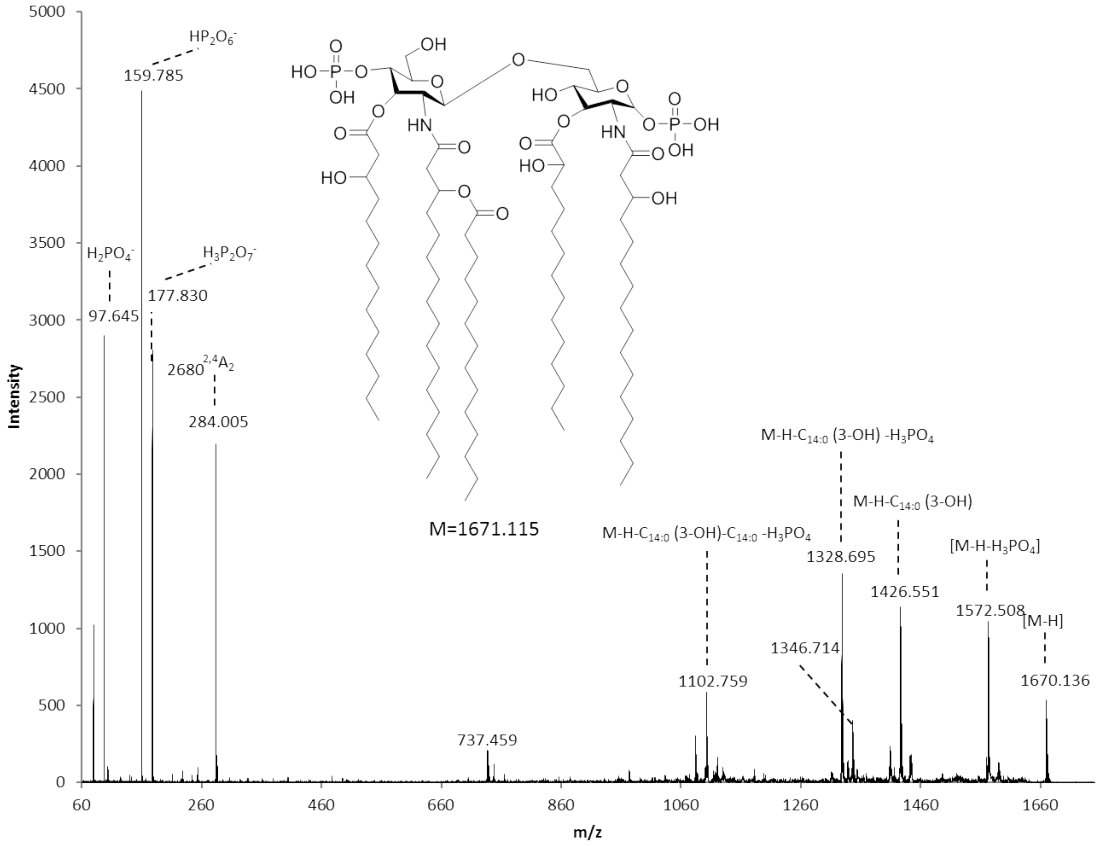

Figure 3-4: A MALDI-MS/MS spectrum of ion with an *m/z* of 1670.135 of lipid A from *B. pseudomallei* 1026b in negative ion mode using ATT as the matrix. Inset: hypothetical structure of the parent lipid A molecule

Loss of H_3PO_4 yields the ion with an *m/z* of 1572.508 and loss of $C_{14:0}$(3-OH) acyl chain results in formation of the ion with an *m/z* of 1426.551. Additional loss of another H_3PO_4 results in an ion with an *m/z* of 1328.695, confirming the presence of two phosphate groups. The ion with an *m/z* value of 1102.759 is due to the loss of one $C_{14:0}$(3-OH), one $C_{14:0}$, and H_3PO_4 from the parent molecule. A cross-ring fragment with an *m/z* value of 284.005 is identified. Presence of two phosphate groups is confirmed by the ions with *m/z* values of 97.645 ($H_2PO_4^-$), and 159.785 ($HP_2O_6^-$).

There are two mechanisms involved in the removal of acyl chains from lipid A: charge-driven process and charge-remote process.[14] Figure 3-5 explains the mechanisms. In charge-driven process, neutral loss of an acyl chain as a ketene derivative is observed, and in the charge-remote process the acyl chain is lost as free fatty acid.[14] For charge-driven process, the presence of phosphate anion at position 4′ was considered very important.[14] The negative charge on the phosphate anion attracts the α-hydrogen of the acyl chain at position 3′. This results in the elimination of acyl chain as a neutral ketene derivative. In charge-remote fragmentation, the negative charge will remain on the phosphate group and it is not involved in the fragmentation.[14] The acyl chains are eliminated as neutral fatty acids.

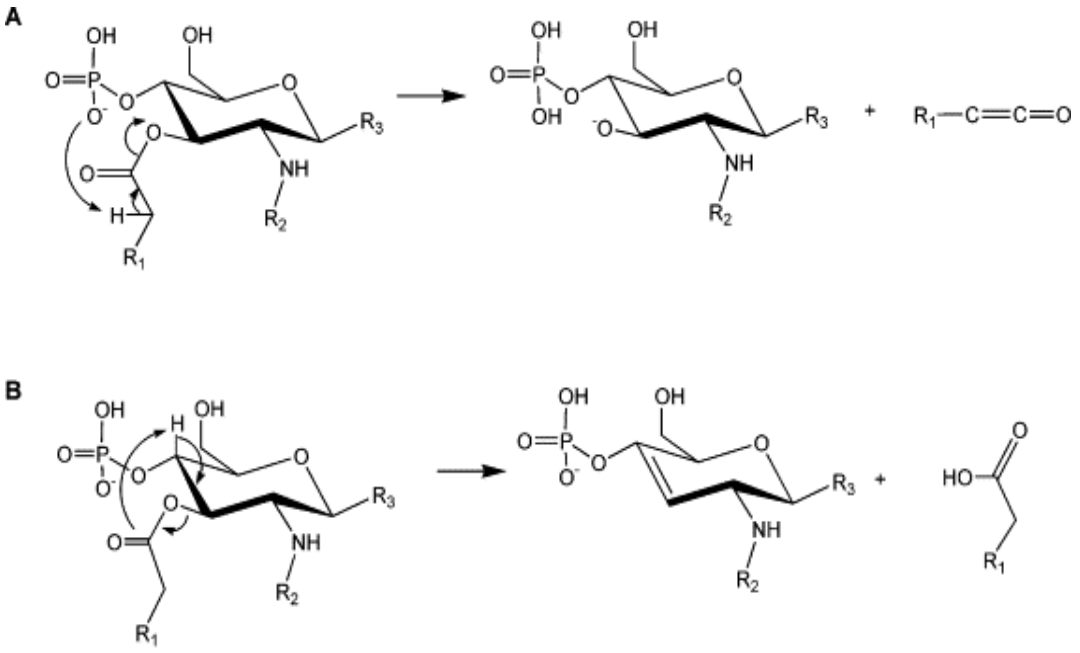

Figure 3-5: Fragmentation mechanisms: (A) Charge-driven fragmentation

(B) Charge-remote fragmentation

Loss of an ester moiety as a free fatty acid and neutral ketene derivative results in formation of two different ions which differ by 18 units. This helps in identifying the acyl chains at position 3′. For example, in the MALDI-MS/MS spectrum of lipid A ion with an *m/z* value of 1670.135 (Figure 3-4), two peaks with a mass difference of 18 are observed at *m/z* values of 1328.695 and 1346.714, indicating that a $C_{14:0}$(3-OH) is lost as free fatty acid and also as a ketene derivative.

The following peaks were assigned in MS/MS data obtained for the parent ion with an *m/z* of 1363.993 (Figure 3-6). The ion with an *m/z* of 1120.433 was due to the loss of the $C_{14:0}$(3-OH) acyl chain. Two cross-ring fragments were also observed with *m/z* values of 747.488 and 807.487, which were assigned as $^{0,2}A_2$ with loss of water and $^{0,4}A_2$ with loss of $C_{14:0}$(3-OH) respectively, using the nomenclature of Domon and Costello.[76]

The presence of the $C_{14:0}$(3-OH) group is confirmed by the presence of the ion with an *m/z* of 244.240. Also, two ions with *m/z* values of 79.610 and 97.630 confirm the presence of phosphate groups (PO_3^- and $H_2PO_4^-$, respectively).

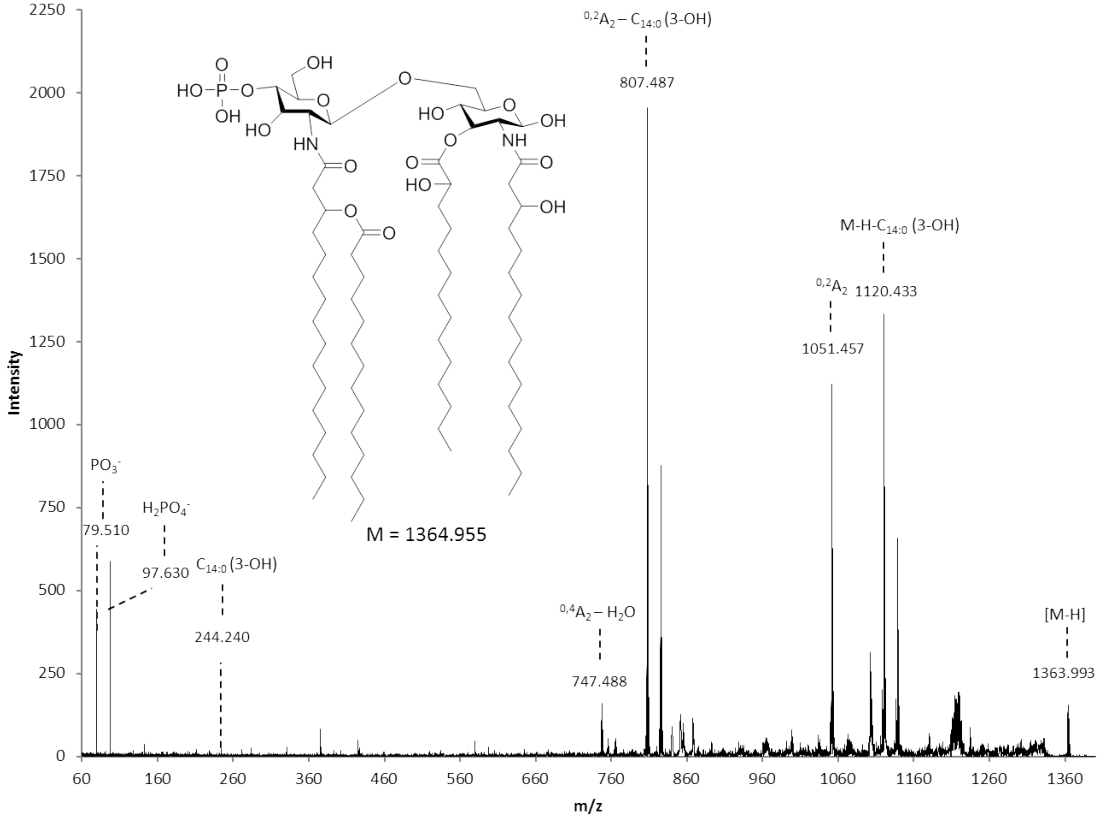

Figure 3-6: A MALDI-MS/MS spectrum of ion with an *m/z* of 1363.993 of lipid A from *B. pseudomallei* 1026b in negative ion mode using ATT as the matrix. Inset: hypothetical structure of the parent lipid A molecule.

MALDI MS/MS spectrum of the ion with an *m/z* of 1580.040 is shown in Figure 3-7. The ions at *m/z* of ~79 (PO_3^-) and 97 ($H_2PO_4^-$) indicate that this lipid A species is phosphorylated. Additionally, the pyrophosphate ion at *m/z* of ~ 159 ($HP_2O_6^-$) indicates that this lipid A species is biphosphorylated.[16]

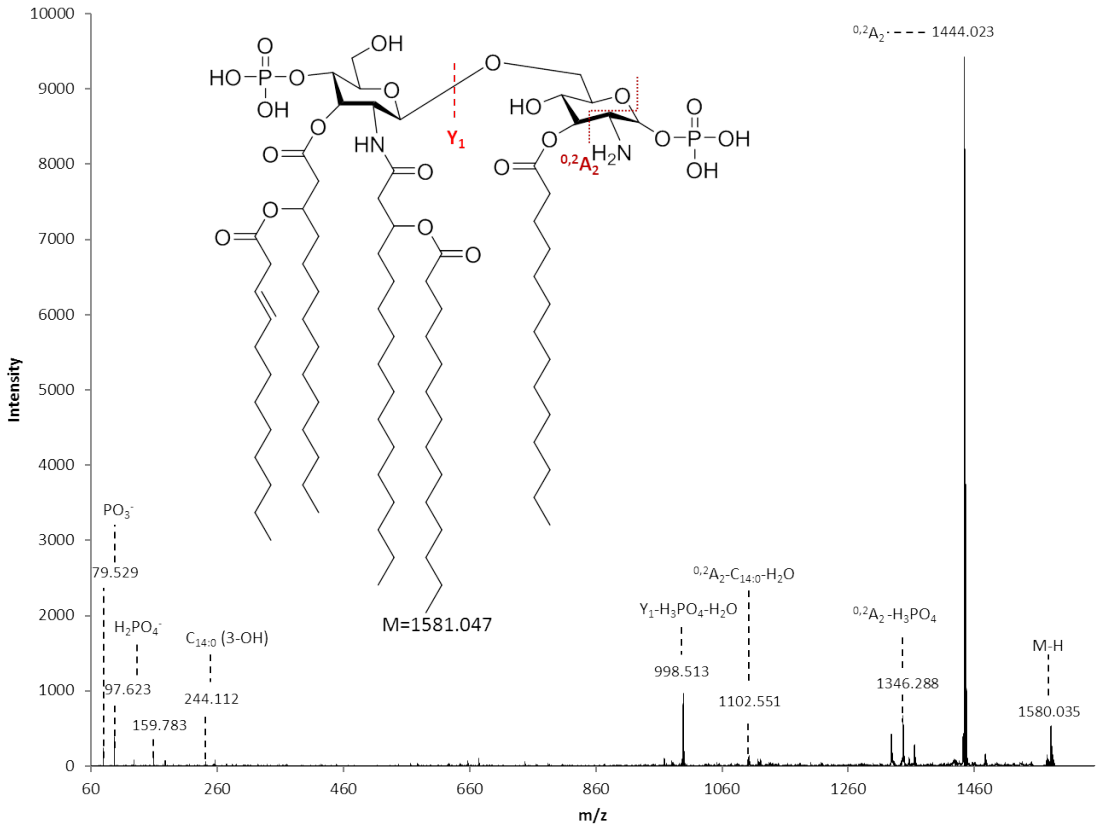

Figure 3-7: A MALDI-MS/MS spectrum of ion with an *m/z* of 1580.040 of lipid A from *B. pseudomallei* 1026b in negative ion mode using ATT as the matrix. Inset: hypothetical structure of the parent lipid A molecule

The most intense fragment ion in the MALDI-MS/MS spectrum of lipid A ion with an *m/z* of 1580 has an *m/z* of ~1444. Since the ion with this *m/z* was detected in *B. pseudomallei* 1026b lipid A spectrum (Figure 3-1), it is interesting to compare MS/MS spectra of ions with *m/z* of 1580 and 1444 (Figures 3-7 and 3-8, respectively). Ions with *m/z* of ~79 (PO_3^-), 97 ($H_2PO_4^-$), and 159 ($HP_2O_6^-$) are very intense in the MS/MS spectrum of 1444, indicating that this ion is also biphosphorylated. Additionally, the

intense fragment ions found in both MS/MS spectra show the same *m/z* values, and can be related to both structures with *m/z* of ~1444 and ~1580.

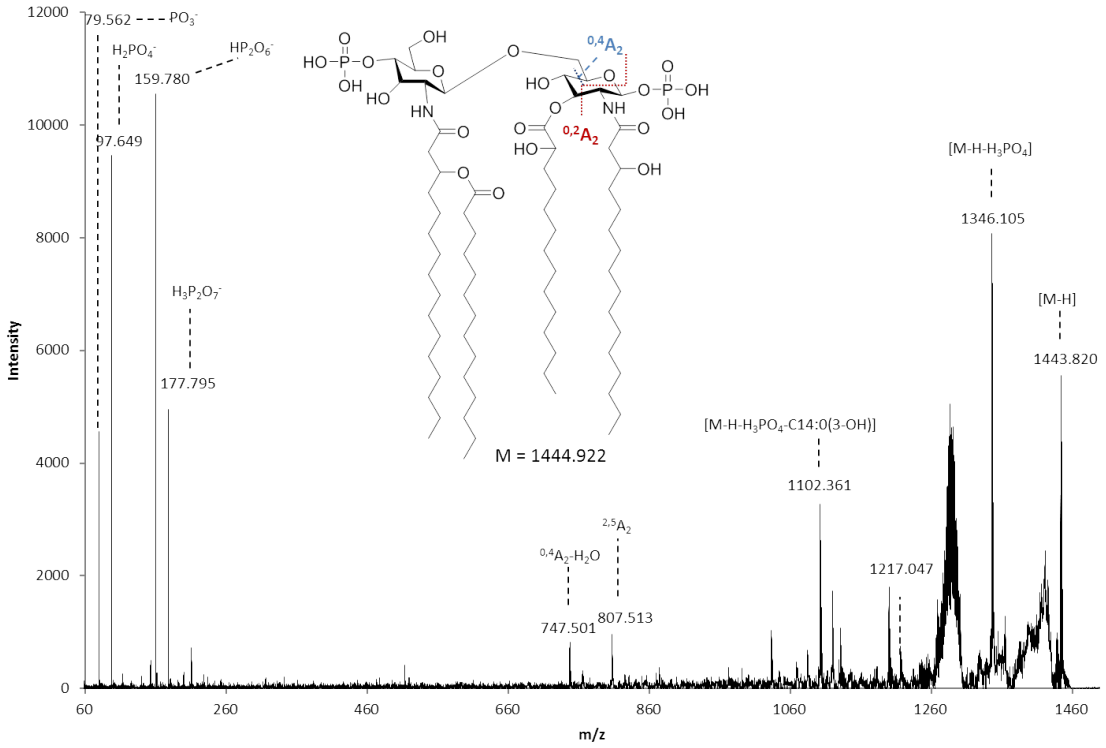

Figure 3-8: A MALDI-MS/MS spectrum of ion with an *m/z* 1443.968 of lipid A from *B. pseudomallei* 1026b in negative ion mode using ATT as the matrix. Inset: hypothetical structure of the parent lipid A molecule

For example, an ion with an *m/z* of ~1346 is likely formed by the neutral loss of phosphoric acid from an ion with an *m/z* of 1444. The ion with an *m/z* of ~1102 is obtained by additional loss of a $C_{14:0}$(3-OH) acyl chain from an ion with an *m/z* of 1346. The ion with an *m/z* of ~1217 is due to the loss of all primary and secondary ester linked acyl chains, which is further confirmed by deacylation studies (described later). In the

MALDI-MS/MS spectrum of the lipid A ion with an *m/z* value of 1580.040, an ion due to glycosidic cleavage along with loss of phosphoric acid and water molecule is observed with an *m/z* value of 998.513. This ion with an *m/z* value of 998.513 is not seen in the MALDI-MS/MS spectrum of the lipid A ion with an *m/z* value of 1443.968.

A cross-ring fragment with an *m/z* of ~747 is also seen in MS/MS spectra of both ions with an *m/z* of 1444 and 1580 but it was low in intensity in the latter spectrum. Based on this data, it can be proposed that the lipid A ion with the *m/z* of ~1580 likely involves a structural motif that has the mass of ~136 Da added to the lipid A structure with an *m/z* of 1444. There are also some fragment ions that are different. There is an ion with an *m/z* of ~807 specific to the lipid A ion with an *m/z* of 1444, and, as mentioned above, an ion with an *m/z* of ~998 is specific to the lipid A ion with an *m/z* of 1580.

In the structure shown in Figure 3-7, the NH_2 group is not acylated, which is not very likely as the amide bonds are strong and not easily fragmented. But, most of the fragments are assigned based on the structure proposed. Also, it was shown in the literature[1, 4] that the main difference between lipid A from *B. pseudomallei* KHW and *B. thailandensis* ATCC 700388 is the presence of the $C_{14:0}$(2-OH) group. Such acyl chain could not be assigned in the structure proposed based on the MS/MS spectra collected.

Figure 3-9 shows another hypothetical structure of the lipid A ion with an *m/z* value of 1580.040 which is isomeric to the structure shown earlier.

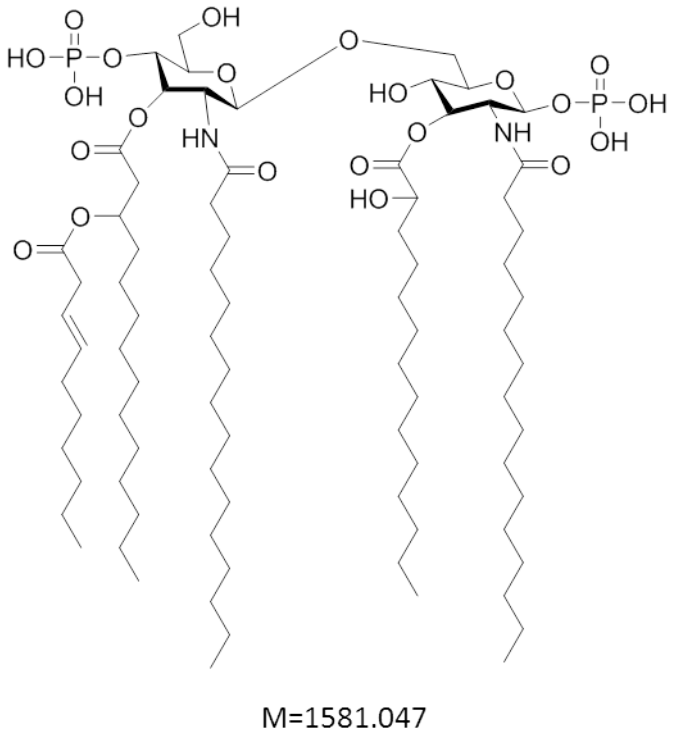

Figure 3-9. Hypothetical structure of the parent molecule of the lipid A ion with an *m/z* value of 1580.040

In the structure shown in Figure 3-9, it can be observed that an amide linked $C_{16:0}$ acyl chain is present. Also, a $C_{14:0}$(2-OH) was incorporated in the structure. However, the major drawback with this structure was inability to assign most of the fragment ions.

As mentioned previously, the lipid A ion, with an *m/z* value of 1580.040 might be a structural modification on lipid A ion with an *m/z* value of 1443.968 since the difference in masses between these two ions is ~136. However, a hypothetical structure with a structural modification on the lipid A ion with an *m/z* value of 1443.968 that results in the formation of a lipid A ion with an *m/z* value of 1580.040, could not be proposed based on acquired MALDI-MS/MS data.

3.2. MALDI-MS and MALDI MS/MS Analysis of O-deacylated Lipid A

The research performed so far on lipid A from *B. pseudomallei* and *B. thailandensis* identified the fatty acid profiles,[1, 4] but exact positions of acyl chains were not confirmed experimentally. To test the acyl chain composition of lipid A species from *B. pseudomallei* 1026b, the O-deacylation study of lipid A samples was performed. Partial and complete O-deacylation of lipid A was performed using ammonium hydroxide and methylamine, respectively. The complete deacylation removed all the ester linked acyl chains, both primary linked and secondary linked O-acyl chains. MALDI-MS spectra obtained after complete deacylation revealed the presence of ions with *m/z* values of 927.591 and 1007.548 (Figure 3-10). The partial deacylation was expected to remove primary ester-linked acyl chains located at positions 3 and 3′ of the lipid A disaccharide backbone.[74] MALDI-MS spectra obtained after partial deacylation of *B. pseudomallei* 1026b lipid A show ions with *m/z* values of 1137.712 and 1217.639 as the most intense peaks (Figure 3-13). MALDI-MS/MS experiments were performed on all four ions from partial and complete deacylation.

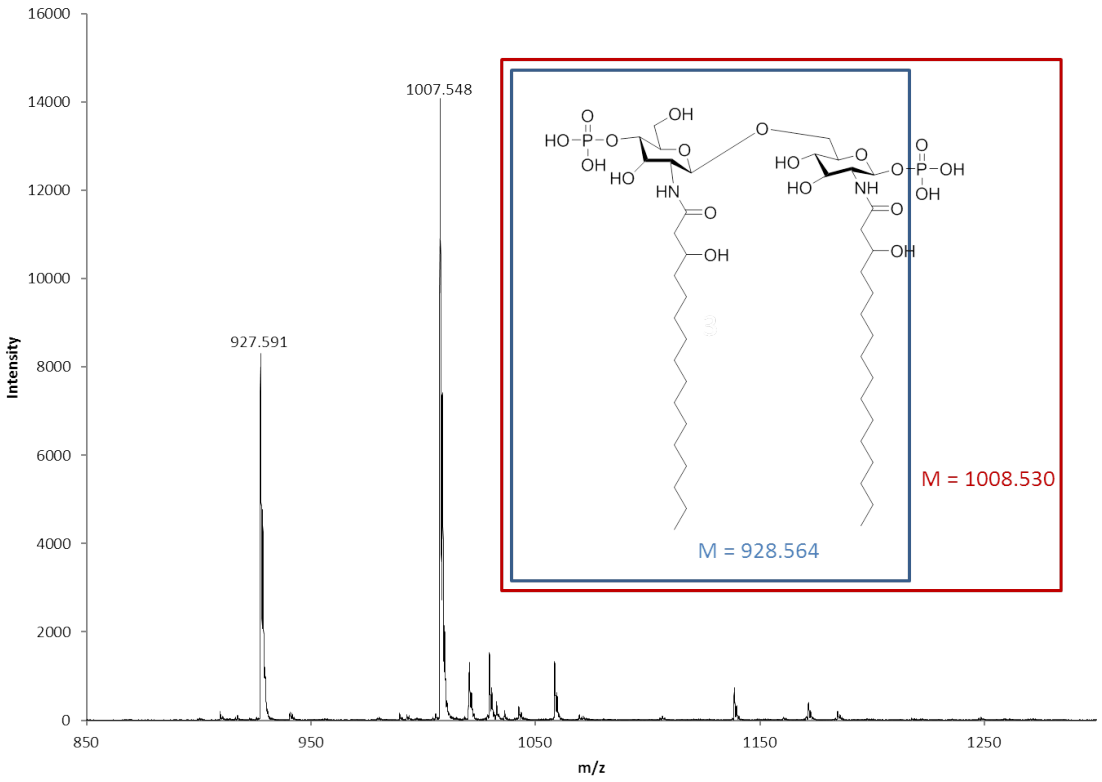

Figure 3-10: A MALDI-MS spectrum of lipid A from *B. pseudomallei* 1026b acquired in negative ion mode using ATT as the matrix after complete O-deacylation using methylamine. Inset: hypothetical structure of the precursor of the ions with *m/z* 927.591 and 1007.548.

From the MS/MS data of the ion with an *m/z* of 927.591 (Figure 3-11), which is due to loss of all ester linked acyl chains from lipid A ion with an *m/z* of 1363.997, different fragment ions were assigned. The ions with *m/z* values of 614.765, 554.801 and 312.911 were assigned as $^{0,2}A_2$, $^{0,4}A_2$, and $^{0,2}X_2$ respectively.

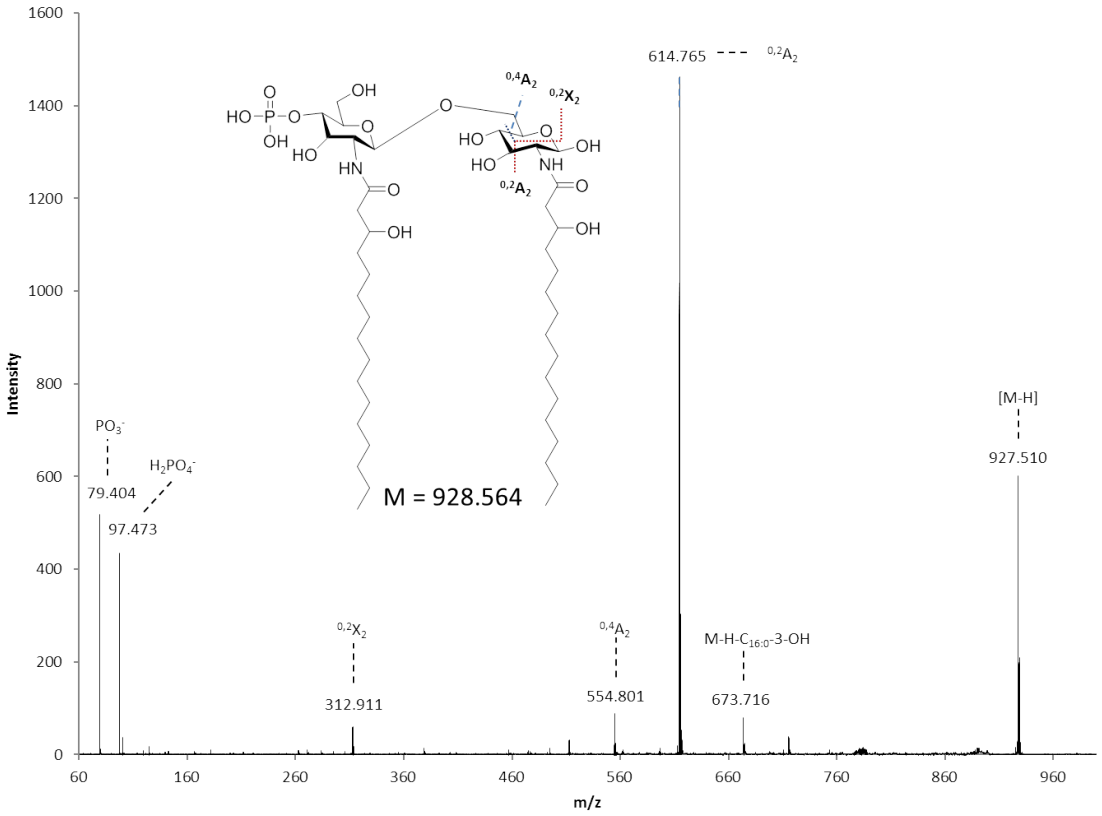

Figure 3-11: A MALDI-MS/MS spectrum of ion with an *m/z* of 927.591 acquired in negative ion mode using ATT as the matrix after complete O-deacylation using methylamine. Inset: hypothetical structure of the parent lipid A molecule

A MALDI-MS/MS spectrum of the ion with an *m/z* of 1007.548 is shown in Figure 3-12. Loss of phosphate group from the deprotonated ion resulted in the formation of ion with an *m/z* value of 909.890. Different cross-ring fragments like $^{2,4}X_2$-$C_{16:0}$, $^{0,2}A_2$-H_2O, and $^{0,4}A_2$, were observed with *m/z* values of 694.386, 596.935, and 554.951 respectively.

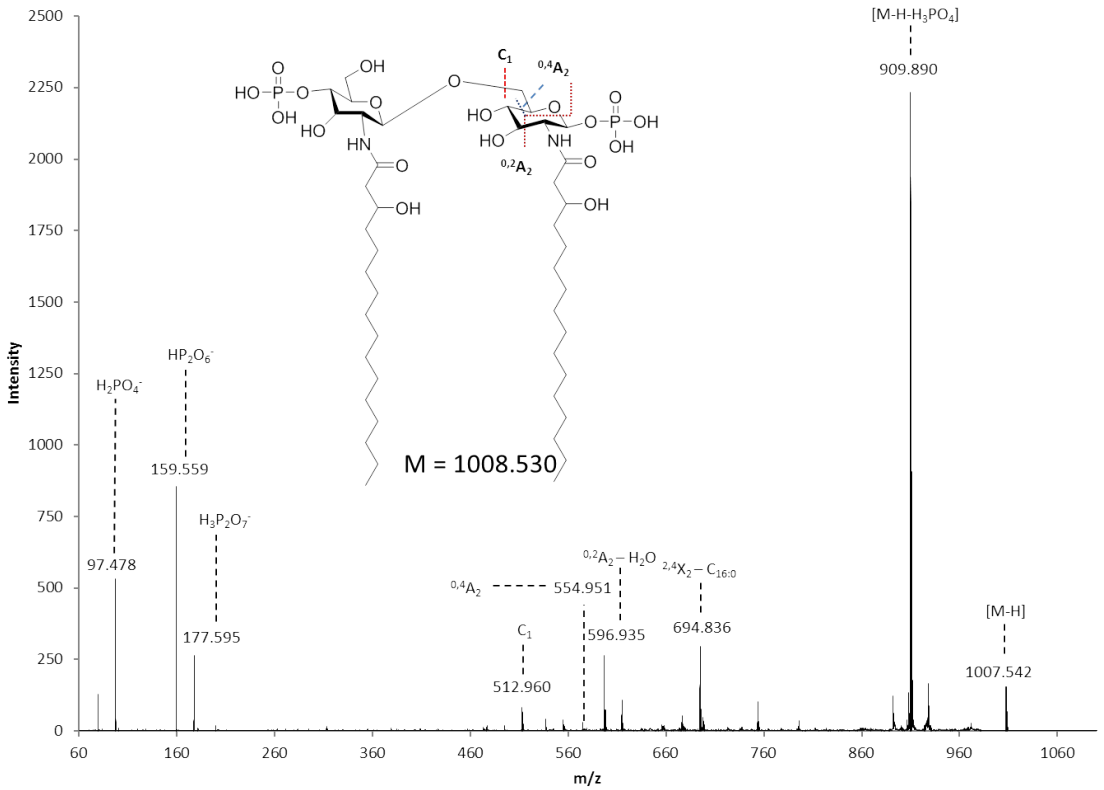

Figure 3-12: A MALDI-MS/MS spectrum of ion with an *m/z* of 1007.548 acquired in negative ion mode using ATT as the matrix after complete O-deacylation using methylamine. Inset: hypothetical structure of the parent lipid A molecule

MALDI-MS data obtained after partial deacylation revealed the presence of three ions with *m/z* values of 1137.712, 1217.639, and 1268.708 (Figure 3-13). The ion with an *m/z* of 1137.712 likely corresponds to the deacylation loss of $C_{14:0}$ acyl chain ($\Delta m/z$ ~ 227) bound by an ester linkage to the lipid A ion with an *m/z* value of 1363.988.

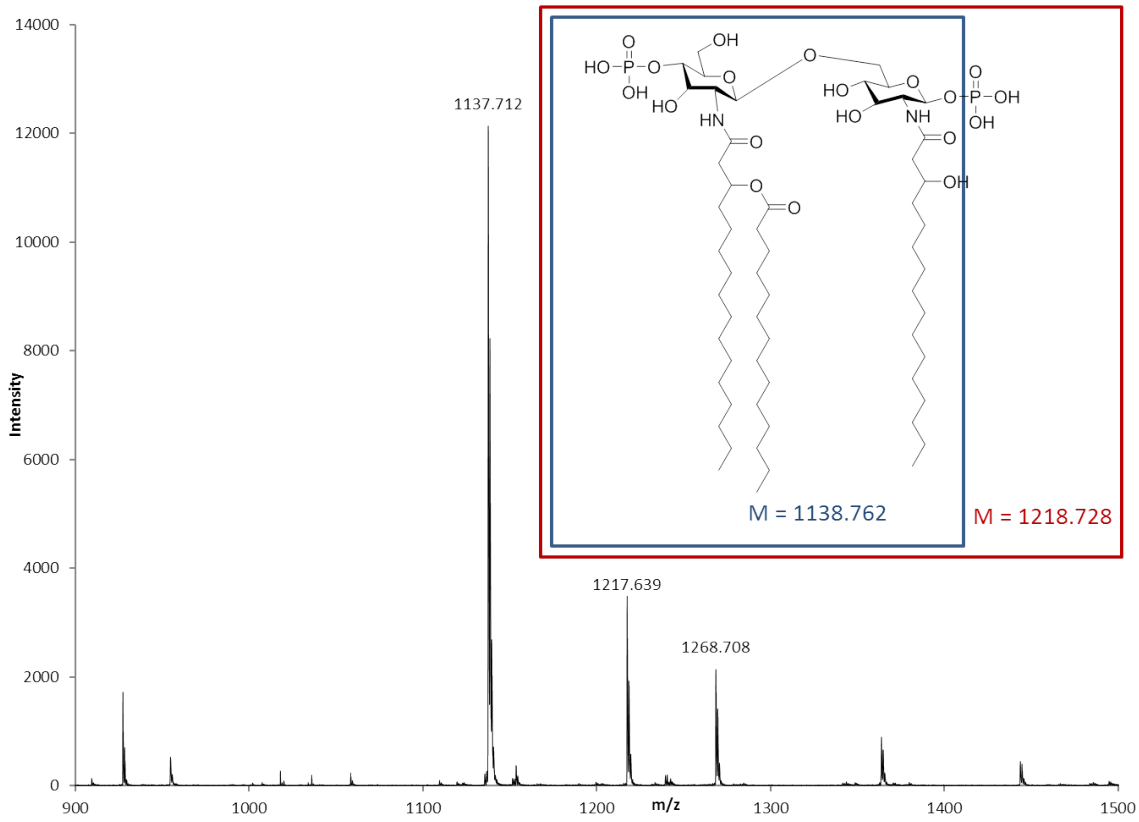

Figure 3-13: A MALDI-MS spectrum of lipid A from *B. pseudomallei* 1026b acquired in negative ion mode using ATT as the matrix after partial O-deacylation using NH_4OH. Inset: hypothetical structures of the precursor of the ions with *m/z* of 1137.712 and 1217.639

The ion with an *m/z* of 1217.639 likely corresponds to the deacylation loss of the $C_{14:0}$ acyl chain bound by an ester linkage to the lipid A ion with an *m/z* value of 1443.968. Also, the ion with an *m/z* value of 1268.708 corresponds to deacylation loss of two $C_{14:0}$ acyl chains bound by an ester linkage and loss of HPO_3 to the lipid A ion with an *m/z* of 1801.231.

A MALDI-MS/MS spectrum of ion with an *m/z* of 1137.712 is shown in Figure 3-14. Loss of a $C_{14:0}$ acyl chain from the parent ion resulted in an ion with an *m/z* of 909.970.

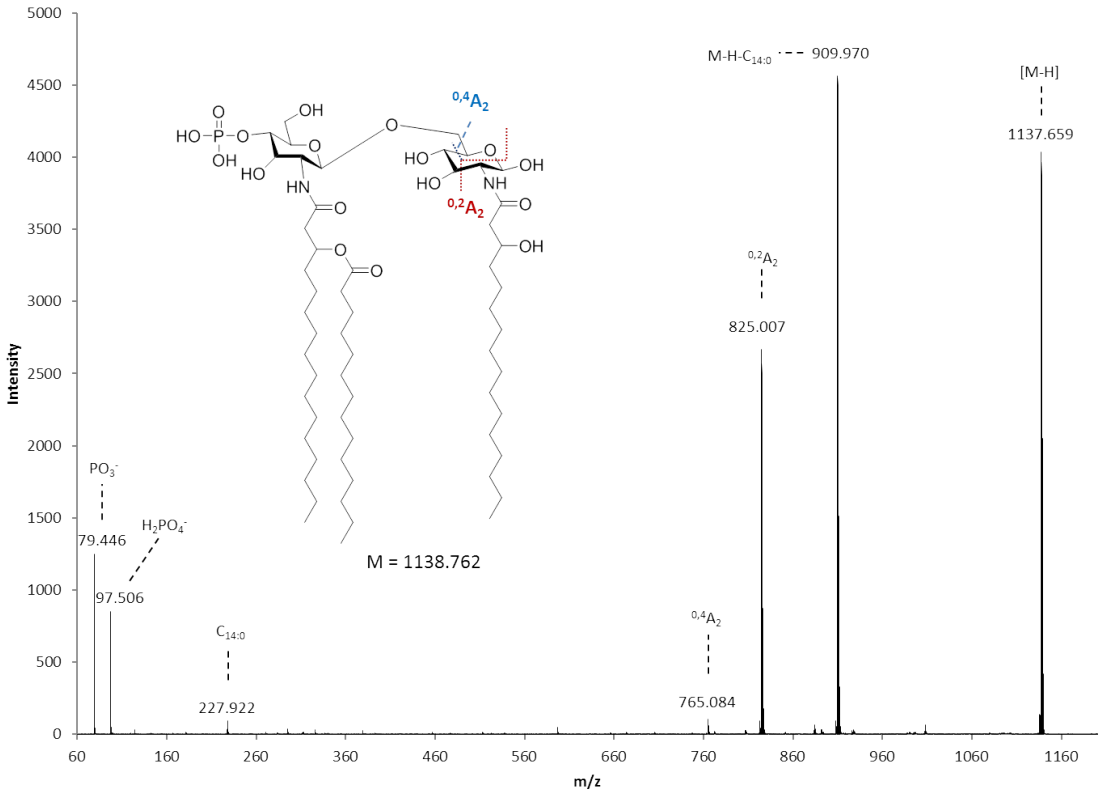

Figure 3-14: A MALDI-MS/MS spectrum of the ion with an *m/z* of 1137.712 acquired in negative ion mode using ATT as the matrix after partial O-deacylation using NH_4OH. Inset: hypothetical structure of the parent lipid A molecule

Two cross-ring fragments that are common were also seen in the spectra with *m/z* values of 825.007 ($^{0,2}A_2$) and 765.084 ($^{0,4}A_2$). The loss of $C_{14:0}$ from 1137.712 is also confirmed by the ion with an *m/z* of 227.922.

MALDI-MS/MS spectra of the ion with an *m/z* of 1217.639 (Figure 3-15) revealed the presence of more cross-ring fragments. $^{0,4}A_2$, $^{2,5}A_2$, and $^{0,4}A_2$, were the cross-ring fragments seen with *m/z* values of 765.413, 807.381, and 825.376 respectively.

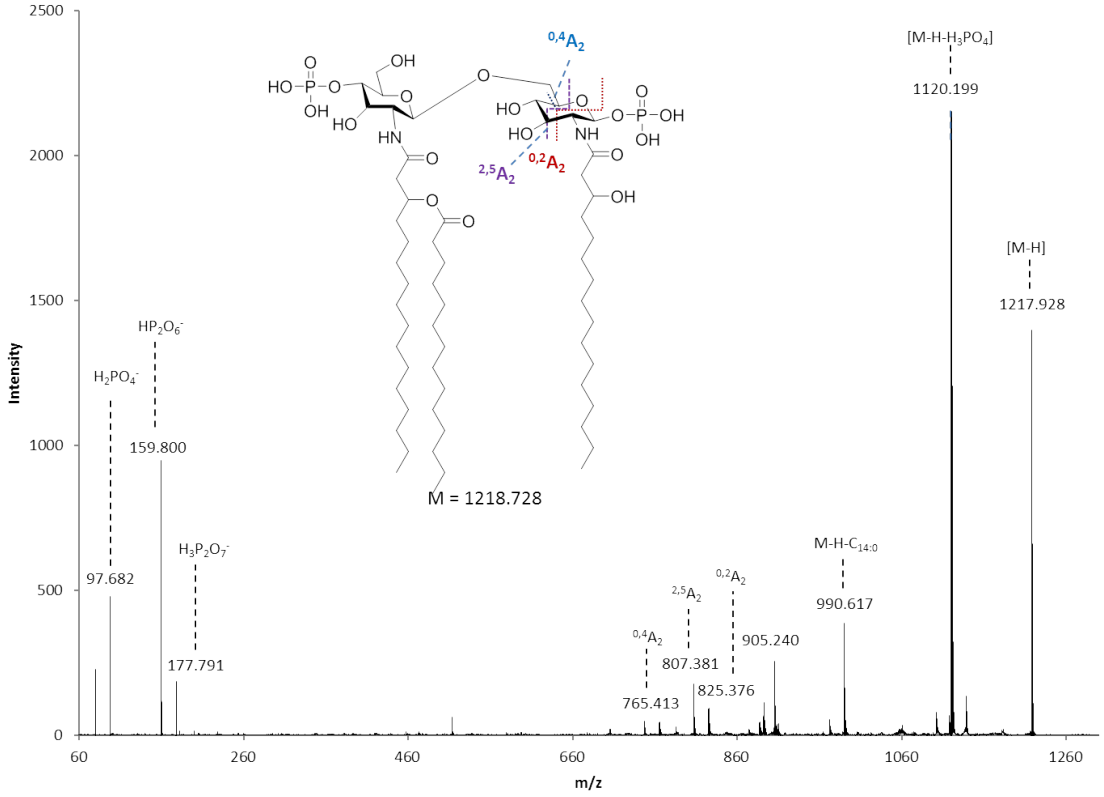

Figure 3-15: A MALDI-MS/MS spectrum of the ion with an *m/z* of 1217.639 acquired in negative ion mode using ATT as the matrix after partial O-deacylation using NH_4OH. Inset: hypothetical structure of the parent lipid A molecule

Based on these cross-ring fragments from all MALDI-MS/MS data obtained after deacylation studies, positions of different acyl chains were confirmed and correspond to those shown by Novem et al. (Figure 1-7).[1] By complete deacylation, a loss of $C_{14:0}$(3-OH) was noticed from the ion with an *m/z* of 1217, which is present as a secondary acyl

chain on an amide-link hexadecanoic acid $C_{16:0}$. While the ion with an *m/z* of 1217 likely originates from partial O-deacylation of the ion with an *m/z* of 1444, it was not possible to detect any ion that would correspond to partial deacylation of the ion with an *m/z* of 1580. Both ions with *m/z* of 1580 and 1444 may yield the same O-deacylation product *(m/z* 1217). This indicates that the structure with a mass of 136 is also cleaved during partial O-deacylation of lipid A ion with an *m/z* of 1580. While neutral loss of 136 was seen in lipids containing phosphatidic acid,[77] it has not been possible to assign additional fragments in the MS/MS spectrum of the ion with an *m/z* of 1580 by adding phosphatidic acid to the lipid A ion with an *m/z* of 1444.

3.3. ESI-MS, ESI-MS/MS, and ESI MS/MS/MS Analysis of Lipid A

To further study the structure of the lipid A with an *m/z* of 1580, lipid A samples were analyzed using ESI-MS. In addition to analysis of ions with an ion trap mass spectrometer (data not shown), high-resolution ESI-MS spectra of lipid A from *B. pseudomallei* 1026b were acquired at Fred Hutchinson Cancer Research Center (Seattle, WA).

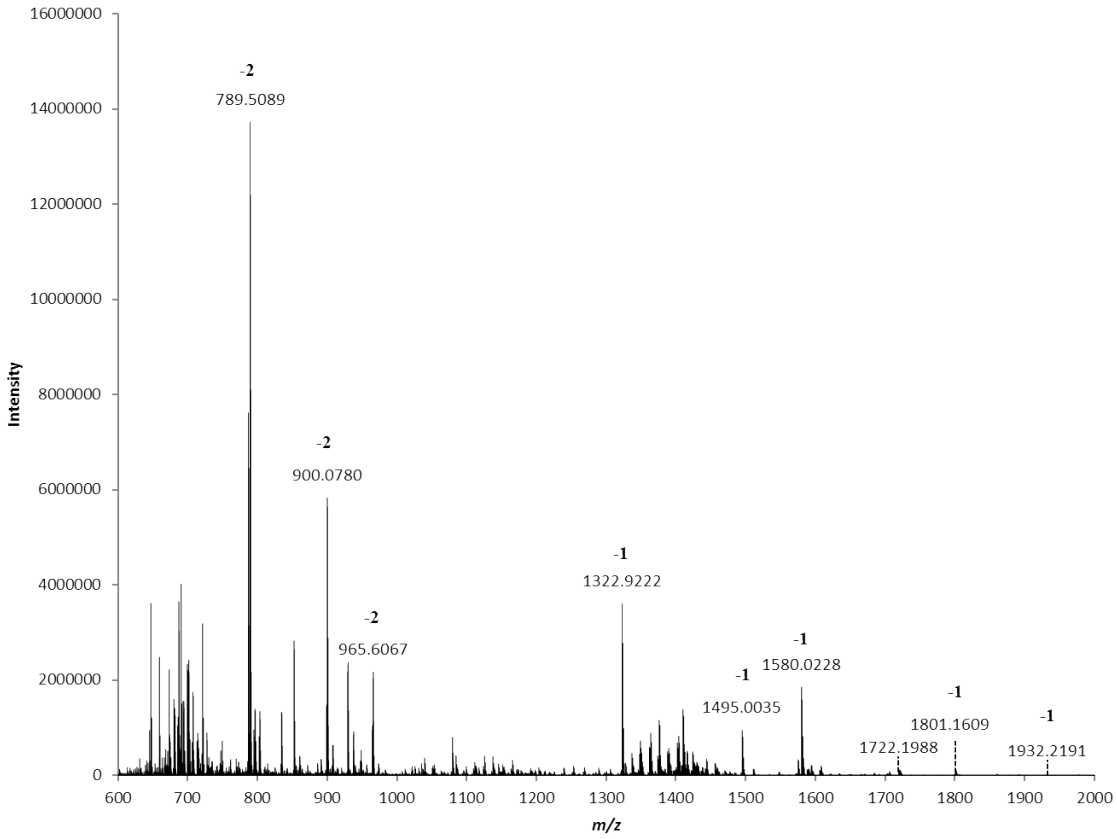

Figure 3-16: A high resolution ESI-MS spectrum of lipid A from *B. pseudomallei* 1026b acquired in negative ion mode

Peaks with *m/z* values of 789.509 (z=-2), 900.078 (z=-2), 1322.922 (z=-1), and 1580.022 (z=-1) were the most intense in ESI-MS spectra (Figure 3-16). The ion with an *m/z* of ~1580 was detected as both a singly and doubly charged ion because it contains two phosphate groups.

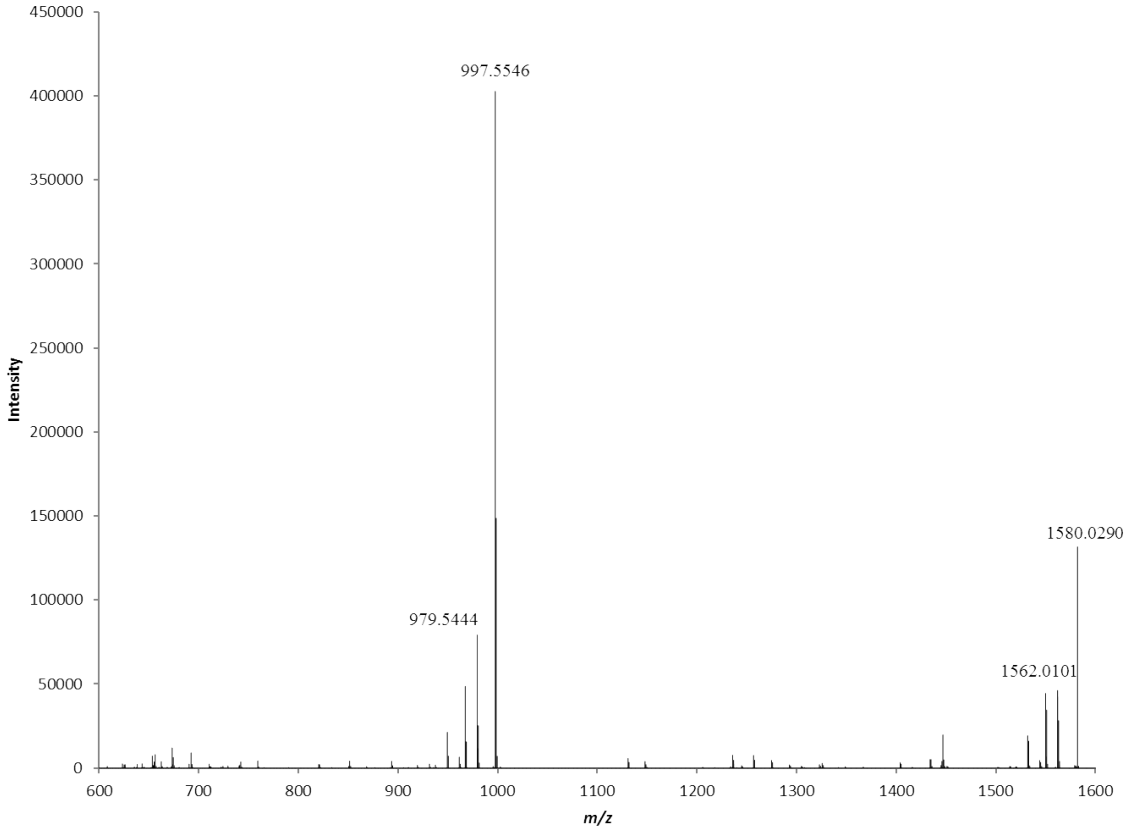

Figure 3-17: A high resolution ESI-MS/MS spectrum of ion with *m/z* 1580.022 of lipid A from *B. pseudomallei* 1026b in negative ion mode

MS/MS and MS/MS/MS analyses were done on singly charged peaks with an *m/z* of 1580 and 997, respectively. The most intense ion in MS/MS spectrum of ion with an *m/z* of 1580 (Figure 3-17) was an ion with an *m/z* of ~998, which was also detected by MALDI MS/MS. However, the ion with an *m/z* of 1444 was absent from the ESI-MS/MS spectrum. This is likely due to different modes of fragmentation in MALDI-MS and ESI-MS instruments (laser induced dissociation vs. high-energy collision-induced dissociation). The neutral loss of water from the ion with an *m/z* of 1580 was also

observed. An MS/MS/MS spectrum of the ion with an *m/z* of 998 also indicated the neutral loss of water. However, no information on acyl chains was obtained by fragmentation of this ion (MS^3 data not shown).

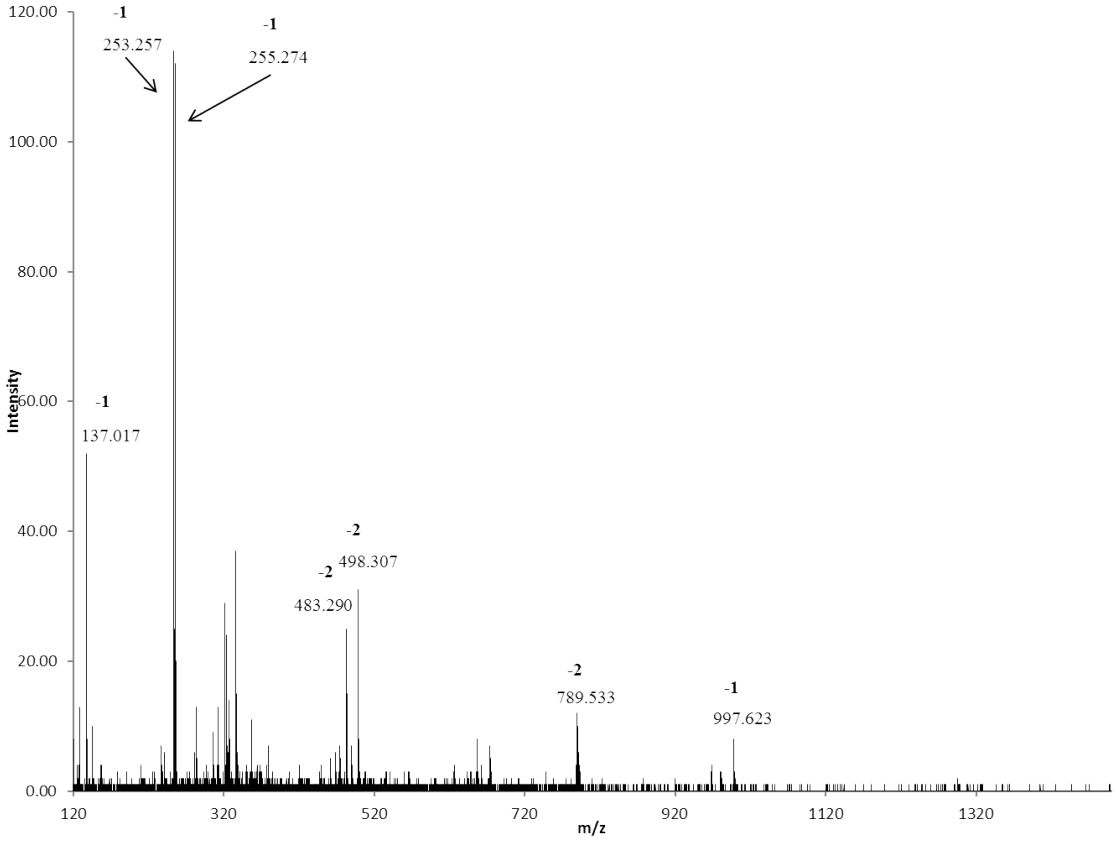

Figure 3-18: A Q-TOF-ESI-MS/MS spectrum of the ion with an *m/z* of 789.5062 of lipid A from *B. pseudomallei* 1026b in negative ion mode

Lipid A samples were also analyzed using Q-TOF-ESI-MS and ESI-MS/MS. MS analysis showed both singly (~1580) and doubly charged (~790) ions of the lipid A ion with an *m/z* of ~1580 (MS data not shown). MS/MS analysis indicated that there might be

a possibility of $C_{16:0}$ and/or $C_{16:1}$ which are represented by *m/z* values of ~ 253 and ~ 255 (Figure 3-18).

Chapter 4

Conclusions and Future Work

4.1 Conclusions

Burkholderia pseudomallei is a virulent bacterium that can have lethal effects. Lipid A, which is a hydrophobic anchor of LPS, has been considered as the main reason for the endotoxic activity of the bacterium.[11] The endotoxic activity of lipid A depends on the degree of acylation and phosphorylation.[58] Structural analyses of lipid A helps in understanding the effects it has on the host's defense system. Therefore, the MALDI-MS and ESI-MS results presented in this thesis are beneficial for studying the virulent properties of *B. pseudomallei* lipid A.

MALDI-MS and ESI-MS data revealed that the virulent *B. pseudomallei* and the avirulent *B. thailandensis* were different from each other as they have slightly different lipid A profiles. Novem et al.[1] described that the difference was due to an additional hydroxyl group at position 2 on a $C_{14:0}$ acyl chain located at position 3 on the disaccharide backbone. In this study it was found that there was another ion which was

different between *B. pseudomallei* 1026b and *B. thailandensis* E264. To account for this difference, a new structure was proposed with an additional $C_{12:1}$ acyl chain to the structure that was proposed by Novem et al.[1] There were other ions that were different between *B. pseudomallei* 1026b and *B. thailandensis* E264, but their intensities were very low and were not reproducible.

For MALDI-MS analysis, matrices like ATT, DHB, and THAP were used to study the structures of lipid A from *B. pseudomallei* 1026b and *B. thailandensis* E264. In this investigation, ATT turned out to be the suitable matrix for lipid A samples. All the data shown for MALDI-MS and MALDI-MS/MS analysis were obtained in negative ion mode using ATT as the matrix. ESI-MS analysis was performed on a Thermo Orbitrap Elite, a Waters Q-TOF, and a Thermo Orbitrap Fusion. MALDI and ESI-MS data were similar except in the case of doubly charged ions that were formed by ESI but not produced using MALDI. However, there were some differences between MALDI and ESI MS/MS data due to different modes of fragmentation used.

Upon analyzing all spectra, it has been concluded that a lipid A species with an *m/z* of 1580.040 (z=-1) is found in lipid A from *B. pseudomallei* 1026b. However, this ion was not observed by MS analysis of lipid A from *B. thailandensis* E264. The presence of two phosphoryl residues on the disaccharide backbone was confirmed by the peaks at *m/z* values of 97.623 and 159.783 in the MALDI-MS/MS spectrum of the lipid A ion with an *m/*z of 1580.040. This species might be a lipid A ion containing two phosphate groups and five acyl chains that are found in the lipid A ion with an *m/z* of 1443.968. Two structures were proposed for the lipid A ion with an *m/z* value of 1580.040. More fragments could be assigned using one structure (Figure 3-7, inset) that

has no acyl chain on the NH_2 group located at position 2 on the disaccharide backbone. From the other structure (Figure 3-9), not many fragments ions were assigned, but it has an amide linked $C_{16:0}$ acyl chain. The lipid A ion with an *m/z* value of 1580.040 could also be some kind of structural modification on lipid A ion with an *m/z* value of 1443.968. This hypothesis is based on the similarities of MS/MS data of lipid A ion with an *m/z* of 1580.040 and lipid A ion with an *m/z* of 1443.968, and will need to be confirmed in future experiments.

To further confirm the structures of the lipid A ions seen in *B. pseudomallei* and *B. thailandensis* E264, deacylation studies were performed. Partial O-deacylation and complete O-deacylation experiments revealed important details about the acylation of lipid A molecules. MS/MS data helped in confirming the hypothetical structures of different lipid A species proposed by Novem et al.[1] From the MS/MS data, different cross-ring fragments were assigned, which helped in confirming the structures. The positions of different acyl chains were confirmed from deacylation experiments and MS/MS experiments. However, the structure of the lipid A ion with an *m/z* of 1580.040 has not been confirmed yet.

4.2 Future Work

Further analyses using techniques such as liquid chromatography-mass spectrometry (LC-MS) and nuclear magnetic resonance (NMR) spectroscopy are needed to determine the exact structure of the lipid A ion with an *m/z* of 1580.040. Ideally, a sufficient amount of lipid A with an *m/z* of 1580.040 should be collected using high performance liquid chromatography (HPLC) separation. If this is achieved, potential

toxic properties of this lipid A structure can be tested in live animal studies and its exact atomic structure can be determined by 2D NMR spectroscopy.[11]

References

1. Novem, V.; Shui, G.; Wang, D.; Bendt, A. K.; Sim, S. H.; Liu, Y.; Thong, T. W.; Sivalingam, S. P.; Ooi, E. E.; Wenk, M. R. Structural and biological diversity of lipopolysaccharides from *Burkholderia pseudomallei* and *Burkholderia thailandensis*. *Clin. Vaccine Immunol.* **2009,** *16* (10), 1420-1428.

2. Leelarasamee, A.; Bovornkitti, S. Melioidosis: review and update. *Rev. Infect. Dis.* **1989,** *11* (3), 413-425.

3. Limmathurotsakul, D.; Dance, D. A.; Wuthiekanun, V.; Kaestli, M.; Mayo, M.; Warner, J.; Wagner, D. M.; Tuanyok, A.; Wertheim, H.; Cheng, T. Y. Systematic review and consensus guidelines for environmental sampling of *Burkholderia pseudomallei*. *PLoS Negl. Trop. Dis.* **2013,** *7* (3), e2105.

4. Li, D.; March, J.; Bills, T.; Holt, B.; Wilson, C.; Lowe, W.; Tolley, H.; Lee, M.; Robison, R. Gas chromatography–mass spectrometry method for rapid identification and differentiation of *Burkholderia pseudomallei* and *Burkholderia mallei* from each other, *Burkholderia thailandensis* and several members of the *Burkholderia cepacia* complex. *J. Appl. Microbiol.* **2013,** *115* (5), 1159-1171.

5. Park, B. S.; Song, D. H.; Kim, H. M.; Choi, B.-S.; Lee, H.; Lee, J.-O. The structural basis of lipopolysaccharide recognition by the TLR4-MD-2 complex. *Nature* **2009,** *458* (7242), 1191-1195.

6. Kilár, A.; Dörnyei, Á.; Kocsis, B. Structural characterization of bacterial lipopolysaccharides with mass spectrometry and on‐and off‐line separation techniques. *Mass Spectrom. Rev.* **2013,** *32* (2), 90-117.

7. O'Brien, J. P.; Needham, B. D.; Henderson, J. C.; Nowicki, E. M.; Trent, M. S.; Brodbelt, J. S. 193 nm ultraviolet photodissociation mass spectrometry for the structural elucidation of lipid A compounds in complex mixtures. *Anal. Chem.* **2014,** *86* (4), 2138-2145.

8. Seydel, U.; Lindner, B.; Wollenweber, H. W.; Rietschel, E. T. Structural studies on the lipid A component of enterobacterial lipopolysaccharides by laser desorption mass spectrometry. *Eur. J. Biochem.* **1984,** *145* (3), 505-509.

9. Rietschel, E. T.; Kirikae, T.; Schade, F. U.; Mamat, U.; Schmidt, G.; Loppnow, H.; Ulmer, A. J.; Zähringer, U.; Seydel, U.; Di Padova, F. Bacterial endotoxin: molecular relationships of structure to activity and function. *The FASEB J.* **1994,** *8* (2), 217-225.

10. Sturiale, L.; Palmigiano, A.; Silipo, A.; Knirel, Y. A.; Anisimov, A. P.; Lanzetta, R.; Parrilli, M.; Molinaro, A.; Garozzo, D. Reflectron MALDI TOF and MALDI TOF/TOF mass spectrometry reveal novel structural details of native lipooligosaccharides. *J. Mass Spectrom.* **2011,** *46* (11), 1135-1142.

11. Zhou, Z.; Ribeiro, A. A.; Raetz, C. R. High-resolution NMR spectroscopy of lipid A molecules containing 4-amino-4-deoxy-l-arabinose and phosphoethanolamine substituents different attachment sites on lipid A molecules from NH4VO3-treated Escherichia coli versus kdsA mutants of *Salmonella typhimurium*. *J. Biol. Chem.* **2000,** *275* (18), 13542-13551.

12. Johnson, R. S.; Her, G.; Grabarek, J.; Hawiger, J.; Reinhold, V. Structural characterization of monophosphoryl lipid A homologs obtained from *Salmonella minnesota* Re595 lipopolysaccharide. *J. Biol. Chem.* **1990,** *265* (14), 8108-8116.

13. Qureshi, N.; Kaltashov, I.; Walker, K.; Doroshenko, V.; Cotter, R. J.; Takayama, K.; Sievert, T. R.; Rice, P. A.; Lin, J.-S. L.; Golenbock, D. T. Structure of the monophosphoryl lipid A moiety obtained from the lipopolysaccharide of *Chlamydia trachomatis*. *J. Biol. Chem.* **1997,** *272* (16), 10594-10600.

14. Kussak, A.; Weintraub, A. Quadrupole ion-trap mass spectrometry to locate fatty acids on lipid A from Gram-negative bacteria. *Anal. Biochem.* **2002,** *307* (1), 131-137.

15. Fukuoka, S.; Knirel, Y. A.; Lindner, B.; Moll, H.; Seydel, U.; Zähringer, U. Elucidation of the Structure of the Core Region and the Complete Structure of the R‐Type Lipopolysaccharide of *Erwinia carotovora* FERM P‐7576. *Eur. J. Biochem.* **1997,** *250* (1), 55-62.

16. Jones, J. W.; Shaffer, S. A.; Ernst, R. K.; Goodlett, D. R.; Tureček, F. Determination of pyrophosphorylated forms of lipid A in Gram-negative bacteria using a multivaried mass spectrometric approach. *Proc. Nat. Acad. Sci.* **2008,** *105* (35), 12742-12747.

17. Boué, S. M.; Cole, R. B. Confirmation of the structure of lipid A from *Enterobacter agglomerans* by electrospray ionization tandem mass spectrometry. *J. Mass Spectrom.* **2000,** *35* (3), 361-368.

18. Chan, S.; Reinhold, V. N. Detailed structural characterization of lipid A: electrospray ionization coupled with tandem mass-spectrometry. *Anal. Biochem.* **1994,** *218* (1), 63-73.

19. Sforza, S.; Silipo, A.; Molinaro, A.; Marchelli, R.; Parrilli, M.; Lanzetta, R. Determination of fatty acid positions in native lipid A by positive and negative electrospray ionization mass spectrometry. *J. Mass Spectrom.* **2004,** *39* (4), 378-383.

20. Que, N. L.; Lin, S.; Cotter, R. J.; Raetz, C. R. Purification and Mass Spectrometry of Six Lipid A Species from the Bacterial Endosymbiont *Rhizobium etli*. Demonstration of a conserved distal unit and a variable proximal portion. *J. Biol. Chem.* **2000,** *275* (36), 28006-28016.

21. Madsen, J. A.; Cullen, T. W.; Trent, M. S.; Brodbelt, J. S. IR and UV photodissociation as analytical tools for characterizing lipid A structures. *Anal. Chem.* **2011,** *83* (13), 5107-5113.

22. Murray, K. K.; Boyd, R. K.; Eberlin, M. N.; Langley, G. J.; Li, L.; Naito, Y. Definitions of terms relating to mass spectrometry (IUPAC Recommendations 2013). *Pure Appl. Chem.* **2013,** *85* (7), 1515-1609.

23. Thomson, J. J. XL. Cathode rays. *Lond. Edinb. and Dubl. Phil.Mag.* **1897,** *44* (269), 293-316.

24. Hoffmann, E. *Mass Spectrometry*. Wiley Online Library: 1996.

25. Hillenkamp, F.; Karas, M.; Beavis, R. C.; Chait, B. T. Matrix-assisted laser desorption/ionization mass spectrometry of biopolymers. *Anal. Chem.* **1991,** *63* (24), 1193A-1203A.

26. Tanaka, K.; Waki, H.; Ido, Y.; Akita, S.; Yoshida, Y.; Yoshida, T.; Matsuo, T. Protein and polymer analyses up to m/z 100 000 by laser ionization time-of-flight mass spectrometry. *Rapid Commun. Mass Spectrom.* **1988,** *2* (8), 151-153.

27. Kim, S.; Ruparel, H. D.; Gilliam, T. C.; Ju, J. Digital genotyping using molecular affinity and mass spectrometry. *Nat. Rev. Genet.* **2003,** *4* (12), 1001-1008.

28. Hillenkamp, F.; Peter-Katalinic, J. *MALDI MS: a practical guide to instrumentation, methods and applications*. John Wiley & Sons: 2013.

29. Hirsch, J.; Hansen, K. C.; Burlingame, A. L.; Matthay, M. A. Proteomics: current techniques and potential applications to lung disease. *Am. J. Physiol. Lung Cell. Mol. Physiol.* **2004,** *287* (1), L1-L23.

30. Karas, M.; Bachmann, D.; Bahr, U. e.; Hillenkamp, F. Matrix-assisted ultraviolet laser desorption of non-volatile compounds. *Int. J. Mass Spectrom. Ion Processes* **1987,** *78*, 53-68.

31. Fenn, J. B.; Mann, M.; Meng, C. K.; Wong, S. F.; Whitehouse, C. M. Electrospray ionization for mass spectrometry of large biomolecules. *Science* **1989,** *246* (4926), 64-71.

32. Wilson, S. R.; Wu, Y. Applications of electrospray ionization mass spectrometry to neutral organic molecules including fullerenes. *J. Am. Soc. Mass Spectrom.* **1993,** *4* (7), 596-603.

33. Hop, C. E.; Bakhtiar, R. Electrospray Ionization Mass Spectrometry: Part III: Applications in Inorganic Chemistry and Synthetic Polymer Chemistry. *J. Chem. Educ.* **1996,** *73* (8), A162.

34. Keith-Roach, M. J. A review of recent trends in electrospray ionization–mass spectrometry for the analysis of metal–organic ligand complexes. *Anal.Chim. Acta* **2010,** *678* (2), 140-148.

35. Cech, N. B.; Enke, C. G. Practical implications of some recent studies in electrospray ionization fundamentals. *Mass Spectrom. Rev.* **2001,** *20* (6), 362-387.

36. Banerjee, S.; Mazumdar, S. Electrospray ionization mass spectrometry: a technique to access the information beyond the molecular weight of the analyte. *Int. J. Anal. Chem.* **2012,** *2012*.

37. Kebarle, P.; Tang, L. From ions in solution to ions in the gas phase-the mechanism of electrospray mass spectrometry. *Anal. Chem.* **1993,** *65* (22), 972A-986A.

38. Gross, J. H. *Mass spectrometry: a textbook*. Springer Science & Business Media: 2004.

39. March, R. E. An introduction to quadrupole ion trap mass spectrometry. *J. Mass Spectrom.***1997,** *32* (4), 351-369.

40. Dole, M.; Mack, L.; Hines, R.; Mobley, R.; Ferguson, L.; Alice, M. d., Molecular beams of macroions. *J. Chem. Phys.* **1968,** *49* (5), 2240-2249.

41. Mack, L. L.; Kralik, P.; Rheude, A.; Dole, M., Molecular beams of macroions. II. *J. Chem. Phys.* **1970,** *52* (10), 4977-4986.

42. Iribarne, J.; Thomson, B. On the evaporation of small ions from charged droplets. *J. Chem. Phys.* **1976,** *64* (6), 2287-2294.

43. Agrawal, P. K.; Bush, C. A.; Qureshi, N.; Takayama, K. Structural analysis of lipid A and Re-lipopolysaccharides by NMR spectroscopic methods. *Adv. Biophys. Chem.* **1994,** *4*, 179-236.

44. Hitchcock, P. J.; Brown, T. M. Morphological heterogeneity among Salmonella lipopolysaccharide chemotypes in silver-stained polyacrylamide gels. *J. Bacteriol.* **1983,** *154* (1), 269-277.

45. Hitchcock, P. J.; Leive, L.; Mäkelä, P.; Rietschel, E. T.; Strittmatter, W.; Morrison, D. Lipopolysaccharide nomenclature--past, present, and future. *J. Bacteriol.* **1986,** *166* (3), 699.

46. Lüderitz, O.; Freudenberg, M. A.; Galanos, C.; Lehmann, V.; Rietschel, E. T.; Shaw, D. H. Lipopolysaccharides of gram-negative bacteria. *Curr. Top. Membr. Trans.* **1982,** *17* (79), 339.

47. Mayer, H.; Bhat, U. R.; Masoud, H.; Radziejewska-Lebrecht, J.; Widemann, C.; Krauss, J. Bacterial lipopolysaccharides. *Pure Appl. Chem.* **1989,** *61* (7), 1271-1282.

48. Westphal, O.; Westphal, U.; Sommer, T. The history of pyrogen research. *Microbiol.* **1977,** *221*.

49. Ribi, E. E.; Cantrell, J. L.; Von Eschen, K. B.; Schwartzman, S. M. Enhancement of endotoxic shock by N-acetylmuramyl-L-alanyl-(L-seryl)-D-isoglutamine (muramyl dipeptide). *Cancer Res.* **1979,** *39* (11), 4756-4759.

50. Galanos, C.; Luderitz, O.; Rietschel, E. T.; Westphal, O.; Brade, H.; Brade, L.; Freudenberg, M.; Schade, U.; Imoto, M.; Yoshimura, H. Synthetic and natural *Escherichia coli* free lipid A express identical endotoxic activities. *Eur. J. Biochem.* **1985,** *148* (1), 1-5.

51. Weinberg, J. B.; Chapman, H. A.; Hibbs, J. B. Characterization of the effects of endotoxin on macrophage tumor cell killing. *J. Immunol.* **1978,** *121* (1), 72-80.

52. Youngner, J. S.; Feingold, D. S.; Chen, J. K. Involvement of a chemical moiety of bacterial lipopolysaccharide in production of interferon in animals. *J. Infect. Dis.* **1973,** *128* (Supplement 1), S227-S231.

53. Ribi, E. E.; Granger, D. L.; Milner, K. C.; Strain, S. M. Brief communication: Tumor regression caused by endotoxins and mycobacterial fractions. *J. Natl. Cancer Inst.***1975,** *55* (5), 1253-1257.

54. Moran, A. P.; Zahringer, U.; Seydel, U.; Scholz, D.; Stutz, P.; RIietschel, E. T. Structural analysis of the lipid a component of *Campylobacter jejuni* CCUG 10936 (serotype O: 2) lipopolysaccharide. *Eur. J. Biochem.* **1991,** *198* (2), 459-469.

55. Zähringer, U.; Lindner, B.; Knirel, Y. A.; van den Akker, W. M.; Hiestand, R.; Heine, H.; Dehio, C. Structure and biological activity of the short-chain lipopolysaccharide from *Bartonella henselae* ATCC 49882T. *J. Biol. Chem.* **2004,** *279* (20), 21046-21054.

56. Wollenweber, H. W.; Broady, K. W.; Luderitz, O.; Rietschel, E. T. The Chemical Structure of Lipid A. *Eur. J. Biochem.* **1982,** *124* (1), 191-198.

57. Rietschel, E. T.; Gotter, H.; LÜDERITZ, O.; Westphal, O. Nature and Linkages of the Fatty Acids Present in the Lipid‐A Component of *Salmonella* Lipopolysaccharides. *Eur. J. Biochem.* **1972,** *28* (2), 166-173.

58. Trent, M. S.; Stead, C. M.; Tran, A. X.; Hankins, J. V. Invited review: diversity of endotoxin and its impact on pathogenesis. *J. Endotoxin Res.* **2006,** *12* (4), 205-223.

59. Erridge, C.; Bennett-Guerrero, E.; Poxton, I. R. Structure and function of lipopolysaccharides. *Microbes Infect.* **2002,** *4* (8), 837-851.

60. Baldridge, J. R.; McGowan, P.; Evans, J. T.; Cluff, C.; Mossman, S.; Johnson, D.; Persing, D. Taking a Toll on human disease: Toll-like receptor 4 agonists as vaccine adjuvants and monotherapeutic agents. *Expert Opin. Biol. Ther.* **2004,** *4* (7), 1129-1138.

61. Guo, L.; Lim, K. B.; Poduje, C. M.; Daniel, M.; Gunn, J. S.; Hackett, M.; Miller, S. I. Lipid A acylation and bacterial resistance against vertebrate antimicrobial peptides. *Cell* **1998,** *95* (2), 189-198.

62. Banoub, J. H.; Aneed, A. E.; Cohen, A. M.; Joly, N. Structural investigation of bacterial lipopolysaccharides by mass spectrometry and tandem mass spectrometry. *Mass Spectrom. Rev.* **2010,** *29* (4), 606-650.

63. Zhou, P.; Altman, E.; Perry, M. B.; Li, J. Study of matrix additives for sensitive analysis of lipid A by matrix-assisted laser desorption ionization mass spectrometry. *Appl. Environ. Microbiol.* **2010,** *76* (11), 3437-3443.

64. Schiller, J.; Arnhold, J.; Benard, S.; Müller, M.; Reichl, S.; Arnold, K. Lipid analysis by matrix-assisted laser desorption and ionization mass spectrometry: a methodological approach. *Anal. Biochem.* **1999,** *267* (1), 46-56.

65. Papac, D. I.; Wong, A.; Jones, A. J. Analysis of acidic oligosaccharides and glycopeptides by matrix-assisted laser desorption/ionization time-of-flight mass spectrometry. *Anal. Biochem.* **1996,** *68* (18), 3215-3223.

66. Schiller, J.; Süß, R.; Arnhold, J.; Fuchs, B.; Lessig, J.; Müller, M.; Petković, M.; Spalteholz, H.; Zschörnig, O.; Arnold, K. Matrix-assisted laser desorption and ionization time-of-flight (MALDI-TOF) mass spectrometry in lipid and phospholipid research. *Prog. Lipid Res.* **2004,** *43* (5), 449-488.

67. Stübiger, G.; Belgacem, O.; Rehulka, P.; Bicker, W.; Binder, B. R.; Bochkov, V. Analysis of oxidized phospholipids by MALDI mass spectrometry using 6-aza-2-thiothymine together with matrix additives and disposable target surfaces. *Anal. Biochem.* **2010,** *82* (13), 5502-5510.

68. Jones, J. W.; Cohen, I. E.; Tureĉek, F.; Goodlett, D. R.; Ernst, R. K. Comprehensive structure characterization of lipid A extracted from *Yersinia pestis* for determination of its phosphorylation configuration. *J. Am. Soc. Mass Spectrom.* **2010,** *21* (5), 785-799.

69. DeShazer, D. Genomic diversity of *Burkholderia pseudomallei* clinical isolates: subtractive hybridization reveals a *Burkholderia mallei*-specific prophage in *B. pseudomallei* 1026b. *J. Bacteriol.* **2004,** *186* (12), 3938-3950.

70. Smith, M. D.; Wuthiekanun, V.; Walsh, A. L.; White, N. J. Quantitative recovery of *Burkholderia pseudomallei* from soil in Thailand. *Trans. R. Soc. Trop. Med. Hyg.* **1995,** *89* (5), 488-490.

71. Wuthiekanun, V.; Smith, M.; Dance, D.; Walsh, A. L.; Pitt, T.; White, N. Biochemical characteristics of clinical and environmental isolates of *Burkholderia pseudomallei*. *J. Med. Microbiol.* **1996,** *45* (6), 408-412.

72. Brett, P. J.; Burtnick, M. N.; Snyder, D. S.; Shannon, J. G.; Azadi, P.; Gherardini, F. C. *Burkholderia mallei* expresses a unique lipopolysaccharide mixture that is a potent activator of human Toll‐like receptor 4 complexes. *Mol. Microbiol.* **2007,** *63* (2), 379-390.

73. Brett, P. J.; Burtnick, M. N.; Heiss, C.; Azadi, P.; DeShazer, D.; Woods, D. E.; Gherardini, F. C. *Burkholderia thailandensis* oacA mutants facilitate the expression of *Burkholderia mallei*-like O polysaccharides. *Infect. Immun.* **2011,** *79* (2), 961-969.

74. Silipo, A.; Lanzetta, R.; Amoresano, A.; Parrilli, M.; Molinaro, A. Ammonium hydroxide hydrolysis a valuable support in the MALDI-TOF mass spectrometry analysis of Lipid A fatty acid distribution. *J. Lipid Res.* **2002,** *43* (12), 2188-2195.

75. Basheer, S. M.; Guiso, N.; Tirsoaga, A.; Caroff, M.; Novikov, A. Structural modifications occurring in lipid A of *Bordetella bronchiseptica* clinical isolates as demonstrated by matrix‐assisted laser desorption/ionization time‐of‐flight mass spectrometry. *Rapid Commun. Mass Spectrom.* **2011,** *25* (8), 1075-1081.

76. Domon, B.; Costello, C. E. A systematic nomenclature for carbohydrate fragmentations in FAB-MS/MS spectra of glycoconjugates. *Glycoconjugate J.* **1988,** *5* (4), 397-409.

77. Hsu, F.-F.; Turk, J. Charge-remote and charge-driven fragmentation processes in diacyl glycerophosphoethanolamine upon low-energy collisional activation: A mechanistic proposal. *J. Am. Soc. Mass Spectrom.* **2000,** *11* (10), 892-899.

Appendix A

LC-MS study of lipid A from *B. pseudomallei* 1026b

Separation of lipid A is considered to be a very difficult process because of its amphiphilic nature. However, methods were developed in the recent past to achieve successful separation of different lipid A species.[1, 2] In this study, we tried to separate various lipid A species from *B. pseudomallei* 1026b. The primary goal of this study was to collect fractions of the lipid A species corresponding to an ion with an *m/z* value of 1580.040, as this ion is not seen in a similar, but avirulent *B. thailandensis* E264 strain.

The separation process was carried out on a Shimadzu high performance liquid chromatography (HPLC) system coupled to Waters Q-TOF mass spectrometer. A C18 column was used for the separation process. The mobile phases used and the gradient followed are shown in the Figure A-1.[2]

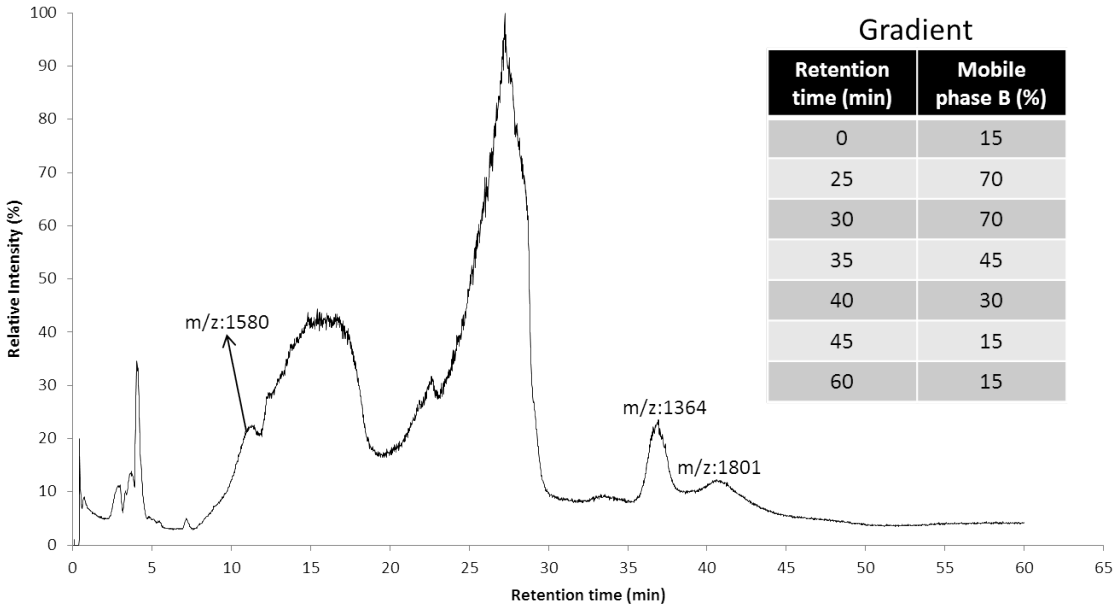

Mobile phase A- 50:50 CH_3OH:H_2O (v/v) with 0.05 % NH_4OH
Mobile phase B- 40:40:20 $CHCl_3$:IPA:CH_3OH (v/v/v) with 0.05 % NH_4OH

Figure A-1: An LC-MS chromatogram of lipid A from *B. pseudomallei* 1026b

Lipid A sample was extracted using a mixture of chloroform, methanol, and water. 20 μL of sample in chloroform/methanol layer was injected into the HPLC system manually using a syringe. From the retention times on the C18 column, it can be said that the ion with an *m/z* value of 1580 is more polar in nature than the lipid A ions with *m/z* values of 1364 and 1801.

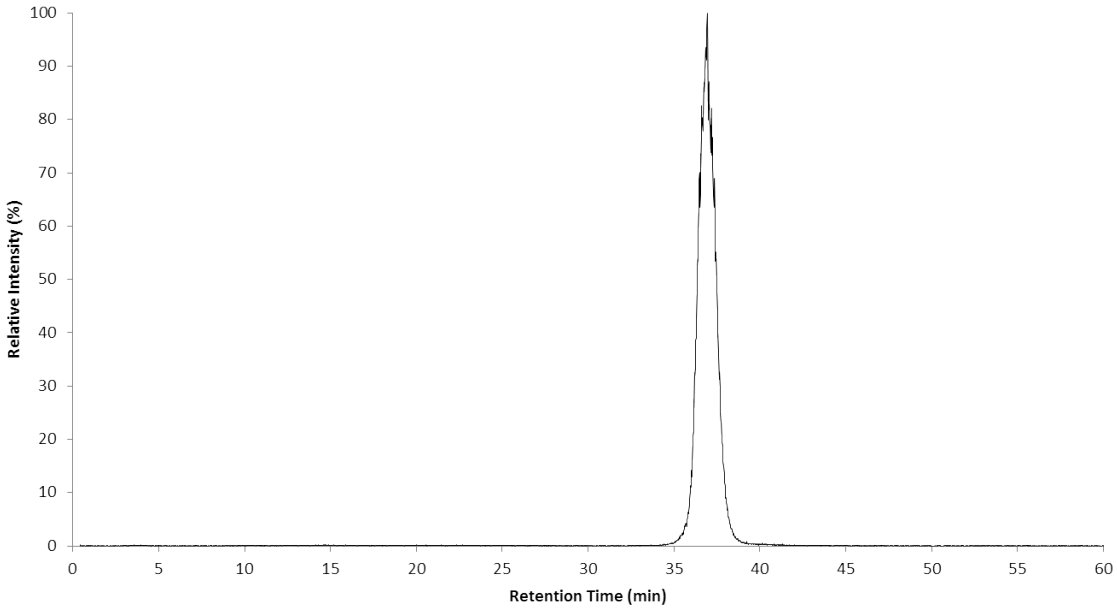

Figure A-2: An extracted ion chromatogram of the lipid A ion with an *m/z* of ~1364 from *B. pseudomallei* 1026b

From the extracted ion chromatogram of the lipid A ion with an *m/z* value of 1364 it can be seen that the retention time of this lipid A ion is between 35 and 40 minutes.

The mass spectrum obtained by integrating the extracted ion chromatogram (Figure A-2) is shown in Figure A-3. It is clearly seen that the peak at an *m/z* value of 1363.8511 is the base peak. The singly and doubly charged ions with *m/z* values of 1574.8873 and 786.9416 are also seen in the spectrum. The ion with an *m/z* of 1574.8873 has an additional $C_{14:0}$ acyl chain than the lipid A ion with an *m/z* value of 1363.8511, but they coelute together.

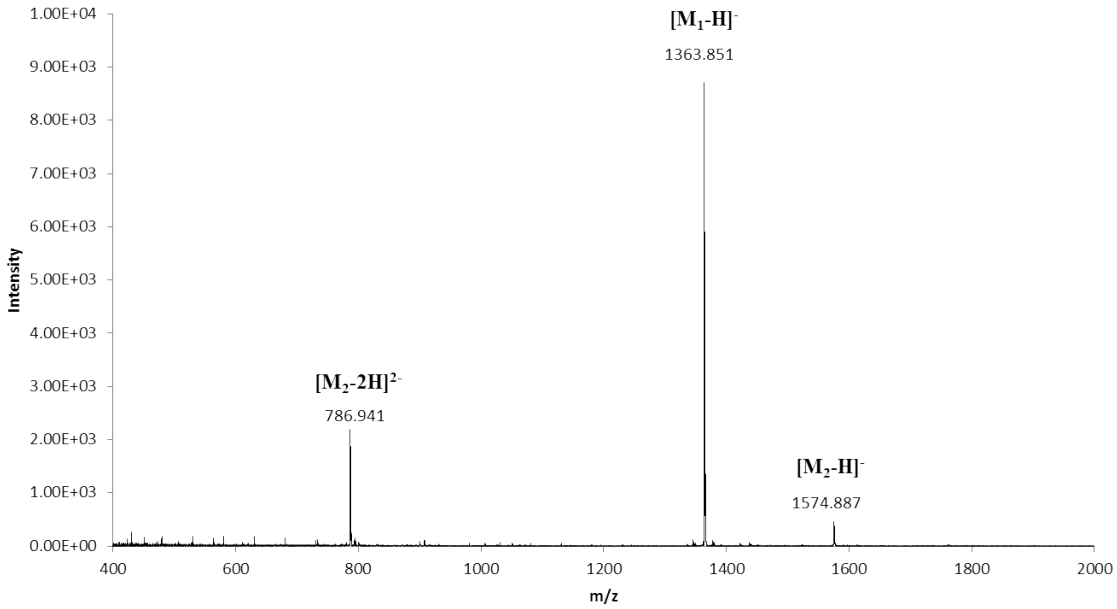

Figure A-3: A mass spectrum of the lipid A ion with an *m/z* of ~1364 from *B. pseudomallei* 1026b

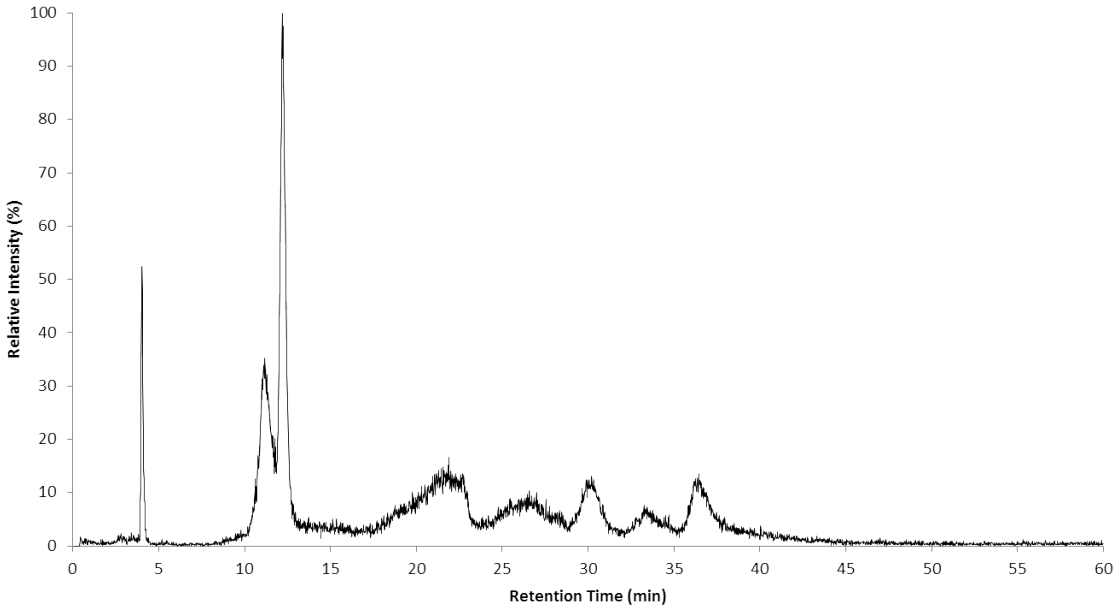

Figure A-4: An extracted ion chromatogram of the lipid A ion with an *m/z* of ~1580 from *B. pseudomallei* 1026b

The extracted ion chromatogram of lipid A ion with an *m/z* value of 1580 is shown in the Figure A-5. From the figure, it is indicated that this lipid A ion is eluted out in the dead volume and also at a retention time of ~ 10-13 minutes.

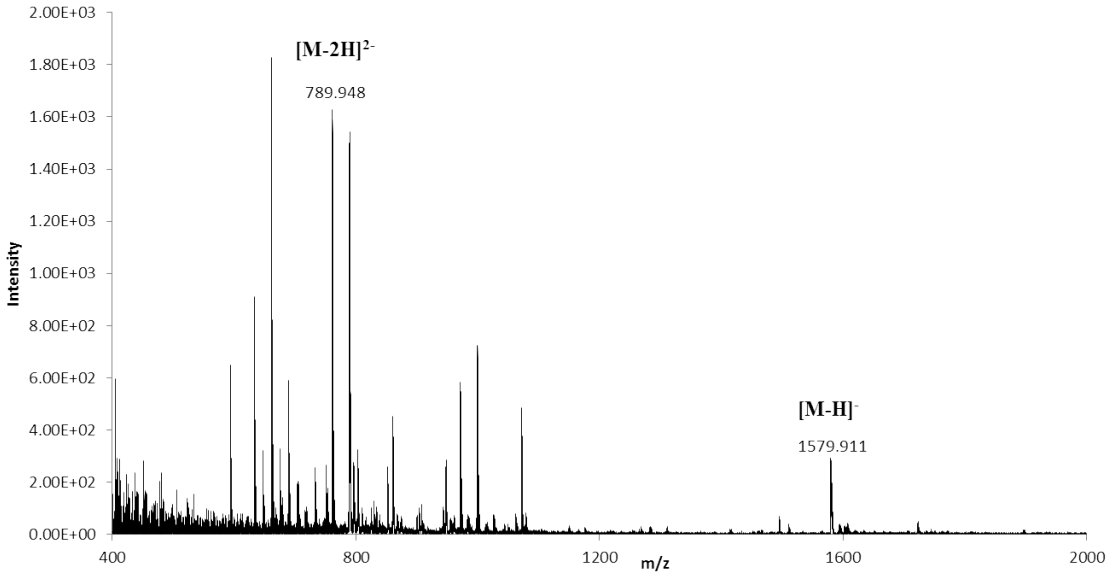

Figure A-5: A mass spectrum of the lipid A ion with an *m/z* of ~1580 from *B. pseudomallei 1026b*

The mass spectrum obtained by integrating the extracted ion chromatogram of the lipid A ion (Figure A-4) at a retention time window between 10 and 15 min is shown in Figure A-5. Singly and doubly charged ions with *m/z* values of 1579.9115 and 789.9486 were observed. There are also peaks which might be due to the presence of impurities in the lipid A.

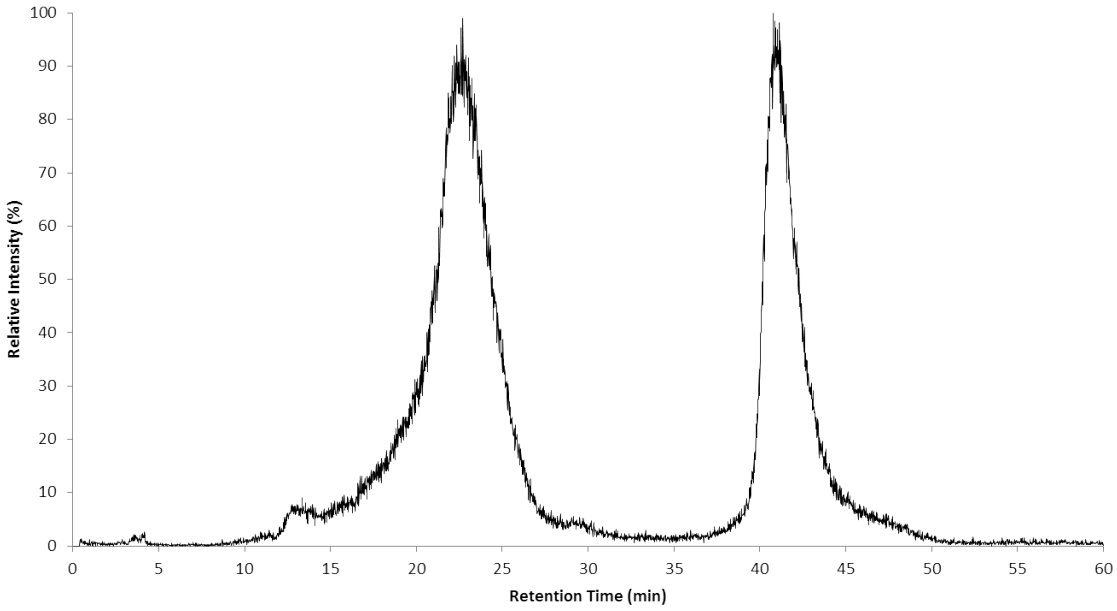

Figure A-6: An extracted ion chromatogram of the lipid A ion with an *m/z* of ~1801 from *B. pseudomallei* 1026b

The extracted ion chromatogram for the lipid A ion with an *m/z* value of 1801 (Figure A-6) indicated that this lipid A ion has two different retention times, one at ~15-26 minutes and another at ~39-45 minutes. The peak at retention time of ~39-45 minutes was integrated to obtain the spectrum of the lipid A ion with an *m/z* value of 1801 (Figure A-7).

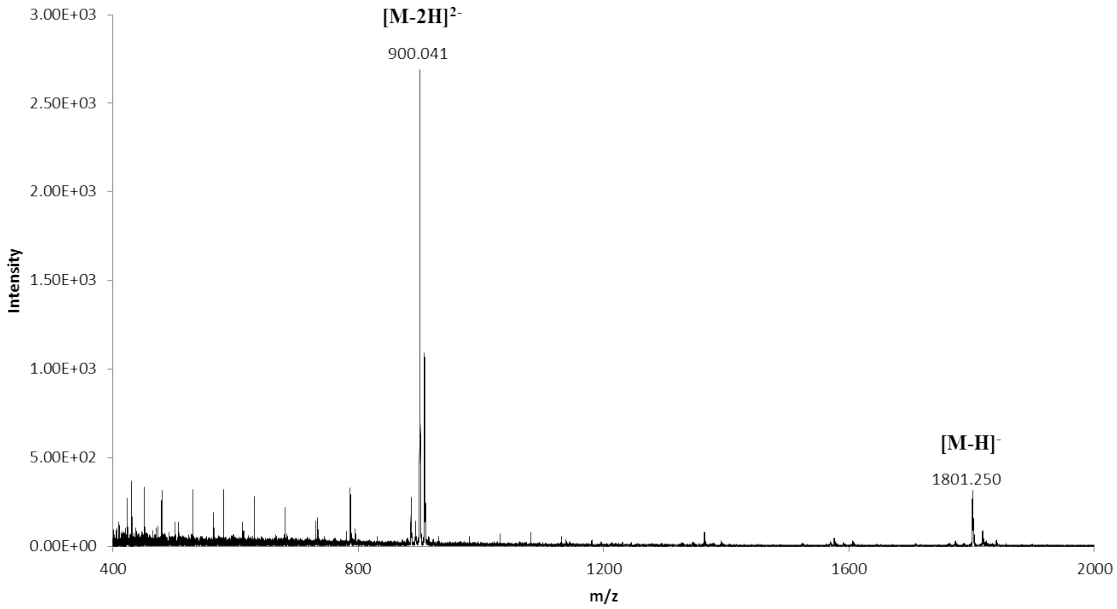

Figure A-7: A mass spectrum of lipid A ion with an *m/z* of ~1801 from *B. pseudomallei* 1026b

The singly and doubly charged ion of the lipid A ion were observed with *m/z* values of 1801.2502 and 900.0411 with the peak at *m/z* of 900.0411 being the base peak. A set of polymer peaks were also identified in the spectrum. As we use chloroform in our mobile phase, it likely deteriorates the peek tubing material, which is indicated by the presence of polymer peaks.

Further experiments should be done using a C8 column in order to obtain better separation of lipid A ions.[2, 3] Such experiments should enable the HPLC purification and further structural characterization of unique lipid A species with an *m/z* of 1580.

References

1. O'Brien, J. P.; Needham, B. D.; Brown, D. B.; Trent, M. S.; Brodbelt, J. S. Top-down strategies for the structural elucidation of intact gram-negative bacterial endotoxins. *Chem. Sci.* **2014,** *5* (11), 4291-4301.

2. O'Brien, J. P.; Needham, B. D.; Henderson, J. C.; Nowicki, E. M.; Trent, M. S.; Brodbelt, J. S. 193 nm ultraviolet photodissociation mass spectrometry for the structural elucidation of lipid A compounds in complex mixtures. *Anal. Chem.***2014,** *86* (4), 2138-2145.

3. Smith, J.; Kaltashov, I. A.; Cotter, R. J.; Vinogradov, E.; Perry, M. B.; Haider, H.; Qureshi, N. Structure of a novel lipid A obtained from the lipopolysaccharide of *Caulobacter crescentus*. *Innate Immun.* **2008,** *14* (1), 25-36.